

**UNIVERSIDADE DE LISBOA**

**FACULDADE DE CIÊNCIAS**

**Departamento de Biologia Vegetal**



**Topoisomerase-II mediated DNA damage: role  
of BRCA1 and other chromatin structure  
regulators**

**Inês Teles Alves**

**Mestrado em Biologia Molecular Humana**

**2009**

**UNIVERSIDADE DE LISBOA**

**FACULDADE DE CIÊNCIAS**

**Departamento de Biologia Vegetal**



**Topoisomerase-II mediated DNA damage: role  
of BRCA1 and other chromatin structure  
regulators**

**Inês Teles Alves**

Dissertação sob orientação científica de:

- Dr. João António Augusto Ferreira  
(Professor associado da Faculdade de Medicina, Universidade de Lisboa)
- Dr. Júlio António Bargão Duarte  
(Professor associado da Faculdade de Ciências, Universidade de Lisboa)

**Mestrado em Biologia Molecular Humana**

**2009**

## Table of contents:

I.	LIST OF FIGURES:.....	I
II.	LIST OF DIAGRAMS AND TABLES: .....	IV
III.	LIST OF ABBREVIATIONS: .....	V
IV.	ACKNOWLEDGMENTS.....	VII
V.	ABSTRACT:.....	IX
VI.	RESUMO:.....	X
VII.	RESUMO ALARGADO: .....	XI
VIII.	KEYWORDS: .....	XIV
IX.	PALAVRAS-CHAVE: .....	XV
I)	INTRODUCTION:.....	- 1 -
II)	OBJECTIVES: .....	- 6 -
III)	MATERIALS AND METHODS:.....	- 7 -
i)	Cell culture: .....	- 7 -
ii)	Drugs, chemicals and antibodies:.....	- 7 -
iii)	Transfection of small hairpin RNA .....	- 8 -
iv)	Western blotting .....	- 8 -
v)	Immunolabeling procedures: .....	- 9 -
vi)	The MTT assay .....	- 10 -
vii)	Clonogenic assay .....	- 10 -
viii)	Flow citometry assay:.....	- 10 -
ix)	Senescence-associated $\beta$ -galactosidade assay:.....	- 10 -

<b>IV) RESULTS:</b> .....	<b>- 11 -</b>
i) Cell line characterization: .....	- 11 -
ii) MTT cytotoxicity assay:.....	- 15 -
iii) Clonogenic assay, the gold standard of cell sensitivity assays:.....	- 17 -
iv) BRCA1 plays a role in triggering the senescent cellular outcome following exposure to Topoisomerase II poisons:.....	- 19 -
v) Time course analysis of the effect of TOP2 and TOP1 drugs in cell cycle distribution and cellular DNA content:.....	- 21 -
a) Etoposide induces a subtle increase in the cellular DNA content:.....	- 21 -
b) BRCA1 knock-down increases the number of cells with high DNA contents after exposure to Doxorubicin.....	- 23 -
vi) The amount of H2A.X lesions is independent of the cell cycle phase at which cells were exposed to Etoposide: .....	- 26 -
vii) Etoposide treatment causes a decrease in histone H3 K9 tri-methylation in addition to an increase in heterochromatin protein 1 $\alpha$ : .....	- 28 -
<b>V) CONCLUSION</b> .....	<b>- 29 -</b>
<b>X. REFERENCES:</b> .....	<b>I</b>
<b>XI. ANNEX</b> .....	<b>V</b>

## I. List of figures:

- Figure 1:** Catalytic mechanism of type II DNA topoisomerases [58].....**v**
- Figure 2:** Schematic illustration of the DNA damage response [59]. Either ATM or ATR can activate signal transduction pathways, which respond to DSBs or to single-stranded regions respectively. The signalling pathways involve mediator proteins that amplify the signal (MDC1, 53BP1, MRN, BRCA1), transducer kinases (CHK1 and CHK2) and effector proteins. There is considerable overlap between ATM and ATR phosphorylation substrates. Two G1/S checkpoints are dependent on ATM signalling.....**v**
- Figure 3:** DNA DSBs repair pathways [29]. Replication forks can stall and may collapse when they encounter a blocking lesion. This will induce H2AX phosphorylation in the site of damage. Fork restart usually involves HR proteins. Fork double strand breaks (two broken ends) may be repaired either by NHEJ or by HR.....**vi**
- Figure 4:** General scheme of DNA damage or replication fork arrest responses: the impact on cell fate, cancer development and genomic instability [34].....**vi**
- Figure 5:** P53-dependent senescence, *adapted from* [60]. An increased DNA damage response results in p53 phosphorylation which transcriptionally upregulates genes that mediate either apoptosis or cellular senescence to inhibit tumorigenesis.....**vii**
- Figure 6:** HCT116 WT growth curve. HCT116 WT cells growing exponentially were plated and counted in a hemocytometer every 12 hours. Results were plotted on a log-linear scale. The population-doubling time was determined using the linear regression equation displayed on the graph. HCT116 WT cell line has a doubling time of 15h and 10 min.....**11**
- Figure 7:** HCT116 p53 K.O. growth curve. HCT116 p53 K.O. cells growing exponentially were plated and counted in a hemocytometer every 11 hours. Results were plotted on a log-linear scale. The population-doubling time was determined using the linear regression equation displayed on the graph. HCT116 p53 K.O. cell line has a doubling time of 16h and 37 min.....**12**
- Figure 8:** HCT116 p21 KO growth curve. HCT116 p21 K.O. cells growing exponentially were plated and counted in a hemocytometer every 11 hours. Results were plotted on a log-linear scale. The population doubling time was determined using the linear regression equation displayed on the graph. HCT116 p21 K.O. cell line has a doubling time of 19h and 46 min.....**12**
- Figure 9:** BrdU labelled mitosis. Cells were stained for BrdU and DNA was stained with DAPI (*bar*, 5µm). Note that BrdU and DAPI colocalize at the metaphasic plate (white arrow). DAPI staining of a metaphasic plate that does not stain for BrdU (grey arrow).....**vii**
- Figure 10:** HCT116 WT labelled mitosis graph. The percentage of mitotic cells BrdU positive (+) at each time point were plotted in the graph and the 50% points in the ascending and descending portions of the curve were determined.....**14**
- Figure 11:** Determination of percentage of survival after doxorubicin treatment. Note that, with 500 nM of doxorubicin, HCT116 WT, HCT116 p53 K.O. and HCT116 p21 K.O. have not yet reached the IC<sub>50</sub>. The percentage of survival with 500 nM of doxorubicin in all three cell lines does not vary significantly.....**16**
- Figure 12:** Determination of percentage survival after irinotecan treatment. Note that, with 3600 nM of irinotecan, HCT116 WT, HCT116 p53 K.O. and HCT116 p21 K.O. have an overall survival close to 70%.....**16**
- Figure 13:** Clonogenic survival assay after doxorubicin treatment. HCT116 BRCA1 k.d. and SCRAMB cells were treated with doxorubicin (500nM, 2h, 4h and 8h) and plated in clonogenic conditions. After one week cells were stained with haematoxylin and counted (both single-cells and colonies). IC<sub>50</sub> for doxorubicin was achieved with 4h exposure to the drug. The increase in % survival with 8h exposure compared to 4h exposure in SCRAMB cells might be a technical artifact. Future experiments shall confirm these results.....**17**

**Figure 14:** Clonogenic survival assay after etoposide treatment. HCT116 BRCA1 k.d. and SCRAMB cells were treated with etoposide (50µM, 10 min, 15 min, 30 min and 45 min) and plated under clonogenic conditions. After one week cells were stained with haematoxylin and counted (both single-cells and colonies). IC<sub>50</sub> for etoposide was achieved with 15 min exposure to the drug. The increase in % survival with 15 min exposure compared to 10 min in both SCRAMB and BRCA1 k.d. cells might be a technical artifact. Future experiments shall confirm these results.....**18**

**Figure 15:** Western blotting experiment to evaluate the level of BRCA1 depletion. HCT116 WT SCRAMB, lane 1 and HCT116 WT BRCA1 k.d., lane 2.....**ix**

**Figure 16:** Haematoxylin staining of HCT116 WT BRCA1 k.d. cells. A, HCT116 WT BRCA1 k.d. cells treated with doxorubicin (500nM, 4h). Note the size of the senescent cell (black arrow). Bar, 60 µm. B, HCT116 WT BRCA1 k.d. cells (control, no treatment). Note a large colony of regular cells. Bar, 60 µm.....**x**

**Figure 17:** Senescent outcome after doxorubicin treatment. SCRAMB and BRCA1 k.d. cells were stained with haematoxylin and classified as either senescent-like or normal looking cells. BRCA1 k.d. cells displayed a significant increase in the proportion of senescent-like cells compared to SCRAMB cells.....**19**

**Figure 18:** Senescent outcome after irinotecan treatment. SCRAMB and BRCA1 k.d. cells were stained with haematoxylin and classified as either senescent-like or normal looking cells. BRCA1 k.d. cells displayed a slight increase in the proportion of senescent-like cells compared to SCRAMB cells.....**20**

**Figure 19:** Senescence-associated β-galactosidase staining of HCT116 WT BRCA1 k.d. cells treated with doxorubicin (500nM, 4h). Bar, 50 µm.....**x**

**Figure 20:** Senescent outcome following etoposide treatment (50 µM, 15 min). Exponentially growing cells were stained for senescence-associated β-galactosidase and imaged by brightfield microscopy using identical image capture settings. For SCRAMB, 785 cells in the control (no treatment) group and 510 in the etoposide group were analysed. For BRCA1 k.d., 978 cells in the control group and 341 in the etoposide group were analysed. BRCA1 k.d. cells displayed an increase of 46% in the senescent outcome compared to SCRAMB cells.....**21**

**Figure 21:** Total DAPI Intensity Histogram. Cells were grown in coverslips and treated with etoposide (50µM, 15 min). DNA was stained with DAPI; ≥ 100 nuclei per experimental group were analysed and distributed according to the total DAPI intensity range. Note that 72h after exposure to etoposide roughly all nuclei were distributed across a wide range of high total DAPI intensities.....**23**

**Figure 22:** Flow cytometry analysis of cell cycle distribution in the controls. . HCT116 WT, p53 K.O. and p21 K.O cell lines with BRCA1 k.d. were designated (BRCA1 k.d. WT, BRCA1 k.d. p53 and BRCA1 k.d. p21 respectively). HCT116 WT, p53 K.O. and p21 K.O cell lines without BRCA1 k.d. were designated (SCRAMB WT, SCRAMB p53 and SCRAMB p21 respectively). Cells growing exponentially were treated with DMSO for 4h, allowed to recover for 1h and then fixed with ethanol 70%. Cells were stained with propidium iodide at least 2h before flow cytometry acquisition. Note that, all BRCA1 k.d. cells displayed a higher number of cells with a mean percentage of DNA content above G2 (%>G2).....**24**

**Figure 23:** Flow cytometry analysis of cell cycle distribution in cells treated with doxorubicin. HCT116 WT, p53 K.O. and p21 K.O cell lines with BRCA1 k.d. were designated (BRCA1 k.d. WT, BRCA1 k.d. p53 and BRCA1 k.d. p21 respectively). HCT116 WT, p53 K.O. and p21 K.O cell lines without BRCA1 k.d. were designated (SCRAMB WT, SCRAMB p53 and SCRAMB p21 respectively). Cells growing exponentially were treated with doxorubicin (500nM, 4h) and fixed with ethanol 70% after 1h, 24h and 48h. Note that, BRCA1 k.d. cells displayed a higher number of cells with a mean percentage of DNA content above G2 (%>G2) compared to SCRAMB cells 48h after treatment with doxorubicin.....**25**

**Figure 24:** FACS analysis of time course cell cycle distribution in cells treated with irinotecan. HCT116 WT, p53 K.O. and p21 K.O cell lines with BRCA1 k.d. were designated (BRCA1 k.d. WT, BRCA1 k.d. p53 and BRCA1 k.d. p21 respectively). HCT116 WT, p53 K.O. and p21 K.O cell lines without BRCA1 k.d. were designated (SCRAMB WT, SCRAMB p53 and SCRAMB p21 respectively). Cells growing exponentially were treated with irinotecan (3600nM, 12h) and fixed with ethanol 70% after 1h, 24h and 48h. Note that, BRCA1 k.d. and SCRAMB cells displayed a similar number of cells with a mean percentage of DNA content above G2 (%>G2) 48h after treatment with Irinotecan.....**26**

**Figure 25:** Use of BrdU-based tag to identify cells that have been damaged at a specific cell cycle phase. To tag cells in early and late S phases, cells were exposed to a BrdU pulse (10µM 15 min) and shortly after (10 min) to etoposide (50µM 15 min). In this way, cells would be exposed to etoposide at early and late S phases and we may analyse them directly by their replication patterns.

To tag cells in G2, cells were exposed to a BrdU pulse and subsequently to etoposide (50µM 15 min) after a 3h chase. The 3h chase was chosen because after 3h, cells that were BrdU-pulsed while in late S phase are in G2 upon exposure to etoposide. Thus, using this chase time, the late S pattern can be used as a marker (“tag”) for targeting G2 stage (i.e. cells targeted by etoposide while in G2).

To tag cells in G1 we have chosen a 7h pulse chase between the BrdU pulse and the etoposide exposure because after 7h cells that were BrdU-pulse while in late S are in G1 upon exposure to etoposide. Similarly, we used the late S pattern as a marker for “tagging” G1 stage.....**27**

**Figure 26:** Cell cycle targeting of H2AX foci after etoposide exposure. Cells were exposed to etoposide (50µM, 15 min) at each cell cycle phase and the levels of H2AX foci were analysed. Cells were imaged by confocal microscopy using identical image capture settings; 25 cells per experimental group were analysed. Note the high dispersion of the H2AX foci area distribution at all cell cycle stages.....**28**

**Figure 27:** Western blot experiment to evaluate the expression levels of HP1α and H3K9me3 in HCT116 WT control (lane 1); HCT116 WT treated with etoposide 50 µM 15 min, 1 day, 2 days and 3 days after exposure (lane 2, lane 3 and lane 4 respectively); HCT116 wt treated with etoposide 50 µM 30 min, 1 day, 2 days and 3 days after exposure (lane 5, lane 6 and lane 7 respectively). MW, molecular weight marker. There was concomitantly an increase in HP1α and a decrease in H3K9me3 after treatment with etoposide.....**29**

## II. List of diagrams and tables:

**Diagram 1:** Schematic of the labelled mitosis method. Cells that were in late S phase when BrdU-pulsed will be the first mitotic BrdU positive (+) cells. Similarly, cells that were in G1 phase when BrdU-pulsed will be the last mitotic BrdU positive (+) cells of the first cell cycle. A second cell cycle will initiate when the original late S phase cells pass through G2 and enter mitosis for the second time.....**ix**

**Diagram 2:** Experimental plan details. Cells growing exponentially were exposed to a short pulse of etoposide (50µM, 15 min) and collected at defined time points (12h, 24h, 48h and 72h after the pulse) for microscopy analysis.....**22**

**Table 1:** Percentage of HCT116 WT mitotic BrdU positive (+) cells at each time point. For each time point approximately 250 cells were analyzed and classified as either BrdU positive (+) or BrdU negative (-). The percentage of mitotic cells BrdU positive (+) was determined for each time point.....**13**

**Table 2:** Absolute duration of each S phase sub-stages in HCT116 WT cell line. For determination of the absolute duration of each S phase sub-stage 264 cells from the 2h time point were classified according to their replication pattern.....**14**



### III. List of abbreviations:

TOP2	DNA topoisomerase II
TOP1	DNA topoisomerase I
TOP2A	DNA topoisomerase II $\alpha$
DSBs	Double-strand breaks
DDR	DNA damage response
PIKKs	Phosphatidylinositol 3-kinase related kinases
ATM	Ataxia Telangiectasia Mutated
ATR	Ataxia Telangiectasia and RAD3-related
DNA-PK	DNA-dependent protein kinase
MDC1	Mediator of DNA damage checkpoint 1
BRCA1	Breast-cancer associated protein 1
53BP1	P53 binding protein 1
MRN	Mre11/Rad50/Nbs1
Mre11	Meiotic recombination 11 protein
Nbs1	Nijmegen breakage syndrome 1
DSE	One-ended DSB
FANCD2	Fanconi anaemia complementation group D2
CHK2	Checkpoint kinase 2
HR	Homologous recombination
NHEJ	Non-homologous end-joining
RPA	Replication protein A
BRCA2	Breast-cancer associated protein 2
SA- $\beta$ gal	Senescence-associated $\beta$ -galactosidase
SAHF	Senescence-associated heterochromatin foci
DAPI	4',6-diamidino-2-phenylindole

HDCAi	Histone deacetylase inhibition
MTT	(3-(4, 5-dimethylthiazolyl-2)-2, 5-diphenyltetrazolium bromide)
HP1	Heterochromatin protein 1
K.O.	Knockout
HCT116 WT	HCT116 wild type for p53 and p21
BrdU	5-bromo-2'-deoxyuridine
IC <sub>50</sub>	Half-minimal inhibitory concentration
SCRAMB	Scramble
k.d.	Knock-down
HP1 $\alpha$	Heterochromatin protein 1 $\alpha$
H3K9me3	Histone H3 tri-methyl K9
DRT	Differential retention of Topoisomerase II

## IV. Acknowledgments

Well it is supposed for me to say in a few words all that has happened in these last eleven months. As you can imagine it is quite difficult to resume such a period of time in mere words as much of what has happened changed the way I am and the way I see things and this kind of effects are not writable. Nevertheless, I will give it a try!

The most dramatic change for me was engaging the scientific world; good lord this is crazy, starting to think and do a thousand things all at the same time without any mess...I know as João says "it is not a patient's life" but for god it is my ass on the line☺! So it turns out that I spent this year quite stressed, worried that I would not be perfect enough doing this, doing that...Nonetheless, here I am a vigorous worker that does her best and learned from the best!

So, I will start thanking to:

- João, the holly João that was always worried about the P.I.B. and saying: "Come on Inês work!" or "You don't have to eat you have to work" or "P.I.B., P.I.B., P.I.B." but the truth is that without his wonderful gourmet chocolates I would not have made it through. Although you were kind of picky sometimes, you always did your best to teach me how to do things properly, how to become a successful scientist, how all these bureaucracies work, how we should be committed to what we are doing with all our heart and our soul. Although we have had a lot of conversations about work and also about life and in many things, especially about life, we do not agree, I have always taken your thoughts in great consideration. Needless is to say how much I thank you for receiving me in your lab and for all your support. You were always available to help me in my search for a PhD and more than that you have prepared me to engage one! In the end, what I really want you to know is that whatever you need in the future, you can count on me for I will do my best to give all your help in return.

- Joana, I have to thank you for all your effort to make me feel at home, with all our nice chats about ourselves and our lives. The way you have treated and trusted in me and in my work made me feel more confident and I can say that it was really a pleasure working with you. Everyday I woke up knowing that we were going to work together was a day I went happier on the bus and went happier home. I will never forget IAJC and I will certainly not forget all you have done for me, all your advices, all your support, all your dedication! You know and even if you don't I want to make it clear that you will always have a home in Holland (in case I go there for my PhD;)

- Pedro, I don't know how I could manage to count all those clonogenic assays without your help! I really have to thank you for helping in everything that I needed. I will go away but whatever I can do for feel free to ask! You know if these "no access to articles" situation continues I will help with the ones I hope I will have access to;)

- Sandra, Ricardo and Joana, I thank you all the support, specially the Ricardo's crazy arabic/japanese things;) Oh and of course "música enrolada" and Joana's nice lunches when all I could eat was lettuce.

- My family, my mother, my sister and my father; my mother and my sister are part of my life, they were always there to support me after an exhausting day at work! I can never thank them enough for that and for all the dedication throughout my entire life! Although my mother got bored every time I talked to her about my work (she couldn't understand a thing) she never stopped listening largely because she enjoyed having company during a two hour's dinner. Well my sister is the only one who does not fall asleep watching cartoons and so I cannot thank her enough for hilarious moments in the cinema. I hope she won't force me to see Hannah Montana! All the dinners at the Chinese, the karaoke, everything we did together helped me to keep a smile on my face in the worst situations. And that's how I will continue as long as Sofia continues to be Hello Kitty fan number one, my mother continues to take hours to finish any meal whatsoever and my father keeps surprising us with wonderful dinners at Edmundo.

- At last but not at least, my boyfriend Rui, to whom I have to thank for everything, all the motivation he gave me when I was so tired and in despair. You know much more than what I may say to you in these acknowledgments; in fact no words can tell what we tell by simply looking at each other. If I say that writing this Master thesis was full of joy and happiness is because you were by my side all along. If I could stand this year in which everything changed it was because you have stood right next to me, the two of us together always. Truthfully this was the first year since we were four years old that our school routine vanished! It was utterly difficult and only we know how much it really affected us; in a glimpse we went from the school chair to the bench table. All the hours we spent talking about such a hasty change made us grow inside and made our relationship grow: we have become more mature. The most valuable treasure we took from this long journey is the strength we have found in each other to "Always look on the bright side of life" and we are always there whatever comes! All the afternoons we have spent chatting and listening to music couldn't have helped us more. Never forget: "everybody's got some trouble when you worry you make it double, don't worry be happy".

## V. Abstract:

DNA topoisomerases are essential to the resolution of DNA topology during several metabolic processes such as transcription, replication and chromosome segregation. Topoisomerase II (TOP2) catalyzes the passage of one DNA double strand through another and that is the reason why this enzyme can (un)knot or (de)catenate DNA molecules. In mammals there are two isoforms of TOP2,  $\alpha$  and  $\beta$ , which are encoded by separate genes. Given their vital functions TOP2 enzymes are a main target of anticancer drugs. Poisons, such as etoposide and doxorubicin, cause DNA double-strand breaks which assault DNA integrity and need to be properly repaired to guarantee genomic stability. The repair of these DNA lesions, either by homologous recombination or non-homologous end joining, will be triggered by the DNA damage response (DDR) in which BRCA1 is one of the key players. Senescence and apoptosis can also be signaled through the DDR, acting as barriers to neoplastic progression. Senescent cells undergo several changes not only in morphology but also in gene expression. Here, we provide evidence that BRCA1 role in the DDR also relates to the cellular fate given that BRCA1 depletion leads to an increase in the senescent outcome following exposure to TOP2 poisons. We also found evidence for etoposide-induced alteration of heterochromatin composition and distribution, namely altered levels of tri-methylated histone H3 at Lysine 9 (H3K9 me3) and heterochromatin protein 1 $\alpha$ . Future studies shall address whether BRCA1 facilitates the senescent outcome via chromatin alteration.

## VI. Resumo:

As DNA topoisomerasas são essenciais para a resolução de alterações na topologia do DNA que surgem das mais diversas actividades metabólicas tais como a transcrição, replicação e segregação dos cromossomas. A enzima DNA topoisomerase II (TOP2) produz quebras transientes na dupla cadeia de DNA através das quais passará a outra dupla cadeia de DNA intacta. Deste mecanismo catalítico resulta a capacidade de catenação/decatenação desta enzima. Os mamíferos possuem duas isoformas da topoisomerase II,  $\alpha$  e  $\beta$ , codificadas por diferentes genes. Em virtude das funções vitais desta enzima, ela é um dos alvos de numerosas drogas utilizadas actualmente no tratamento do cancro. Venenos tais como o Etoposido e a Doxorubicina provocam quebras na dupla cadeia de DNA que precisam de ser convenientemente reparadas de modo a assegurar a estabilidade genómica. A reparação destas lesões, seja por recombinação homóloga ou por junção de extremidades não-homólogas, é iniciada através de uma via de sinalização geral designada: resposta a lesões no DNA. A proteína BRCA1 é um interveniente fulcral nesta resposta onde também se dita o destino celular, senescência ou apoptose a fim de travar a tumorigenese. As células senescentes passam por várias alterações, tanto a nível morfológico como a nível da expressão génica. Verificou-se que o papel de BRCA1 na resposta a lesões no DNA também está relacionado com a decisão sobre o destino celular dado que a depleção de BRCA1 levou a um aumento na senescência após o tratamento com venenos de TOP2. Viu-se também que a trimetilação da histona H3 na lisina 9 diminui após o tratamento com o Etoposido enquanto que a expressão da proteína 1 $\alpha$  da heterocromatina aumenta. Sugerimos assim que BRCA1 influencia a senescência após tratamento com venenos de TOP2 e que tal poderá estar relacionado com modificações estruturais e funcionais da cromatina.

## VII. Resumo Alargado:

A replicação, transcrição, recombinação e a segregação cromossómica são algumas das várias actividades metabólicas que requerem a resolução de topologias complexas no DNA. Na verdade, é a própria estrutura em dupla hélice da molécula de DNA que leva ao surgimento de alterações topológicas durante o seu metabolismo, e garantir a viabilidade celular está dependente da sua resolução. Existe, para esse fim, uma família de enzimas ubíquas: as DNA topoisomerases. Estas enzimas dividem-se em dois tipos: topoisomerases do tipo I, que produzem quebras transientes de cadeia simples no DNA por onde se dá a passagem da cadeia complementar e topoisomerases do tipo II que produzem quebras transientes de cadeia dupla. As diferenças no mecanismo catalítico destas enzimas leva a que possuam diferentes competências, sendo as do tipo I responsáveis principalmente pelo relaxamento dos enrolamentos no DNA e as do tipo II pela actividade de catenação/decatenação. Posto isto, é importante referir que apesar das topoisomerases do tipo II (TOP2) poderem substituir as funções das do tipo I, o inverso já não se aplica uma vez que a actividade de catenação/decatenação é exclusiva das TOP2. Os mamíferos possuem duas isoformas da topoisomerase II,  $\alpha$  e  $\beta$ , codificados por genes distintos.

A importância da TOP2 na viabilidade celular possibilitou a utilização corrente de drogas contra esta enzima no tratamento de vários tipos de cancro. Estas drogas dividem-se em duas grandes classes: venenos, nomeadamente o Etoposido, e a Doxorubicina, e inibidores catalíticos. Enquanto os venenos provocam quebras na dupla cadeia de DNA, os inibidores catalíticos apenas inibem a actividade da enzima não agredindo directamente a integridade genómica. O tratamento com venenos de TOP2 tem inúmeras consequências a nível celular tais como a alteração da expressão génica e a interrupção temporária do ciclo celular. No entanto, é a activação da resposta a lesões no DNA que permite sinalizar a sua reparação quer por recombinação homóloga, quer por junção de extremidades não-homólogas. Esta resposta pode dividir-se em três fases principais: a detecção da lesão de dupla cadeia por proteínas sensores, o recrutamento de proteínas que transduzem o sinal e levam à sua amplificação e finalmente, a mobilização de proteínas efectoras que regulam diversos aspectos funcionais da célula incluindo a reparação do DNA. BRCA1 é uma das proteínas chave desta resposta tendo já sido descritas as suas funções não só ao nível do recrutamento como também de mobilização de outras proteínas. Além disso, BRCA1 também desempenha um papel central na escolha do mecanismo de reparação uma vez que dependendo da fase do ciclo em que a célula se encontra assim deverá ser favorecida a recombinação homóloga ou a junção de

extremidades não-homólogas. BRCA1 participa nos dois mecanismos de reparação mencionados; qualquer defeito ao nível dos mesmos pode causar instabilidade genómica e levar à tumorigenese. De forma a travar estes dois processos a resposta a lesões no DNA pode também levar à apoptose ou à senescência celular através da activação de p53. Na verdade, já se observou em fibroblastos senescentes a persistência de marcadores moleculares característicos da resposta a lesões no DNA, o que vem reforçar ainda mais a ligação entre resposta a lesões no DNA e senescência.

A senescência é descrita como um estado de paragem permanente do ciclo celular no qual a célula sofre várias alterações, tanto a nível morfológico como a nível da expressão génica mantendo-se no entanto metabolicamente activa. Este fenómeno pode ter diversas causas, sendo a resposta a lesões no DNA apenas uma delas. Alterações na estrutura da cromatina também já são reconhecidas como potenciais desencadeadores deste destino celular uma vez que algumas células senescentes possuem focos de heterocromatina associados à senescência. Estes correspondem a heterocromatina facultativa e possuem muitas vezes algumas modificações de histonas (por exemplo a metilação na histona H3 da lisina 9) e proteínas (nomeadamente proteína 1 $\alpha$  da heterocromatina) associadas à heterocromatina. Em oposição a este papel da heterocromatina no estabelecimento e manutenção do estado senescente surge a evidência de que, a utilização de inibidores de acetilases de histonas que promovem a formação de eucromatina, também induzem a senescência; na verdade, núcleos de maiores dimensões, muitas vezes preditivos da senescência, apresentam uma cromatina mais laxa.

Apesar de todos os benefícios que a indução da senescência possa ter como mecanismo inibidor da progressão neoplásica, o facto das células senescentes secretarem factores muitas vezes estimuladores da tumorigenese, e segundo novas evidências, serem capazes de reverter o fenótipo senescente levanta grandes questões sobre o que está realmente estamos a provocar quando recorremos a tratamentos com drogas como venenos de TOP2.

Assim, é nosso objectivo esclarecer de que modo o tratamento com venenos de TOP2 pode conduzir à senescência e, em particular, se BRCA1, dada a sua importância na resposta a lesões no DNA, tem alguma influência neste processo. Além disso, dado que a cromatina parece ter também um papel determinante na senescência, avaliou-se a expressão de histonas modificadas – H3 trimetilada na lisina 9 e proteínas associadas à heterocromatina - proteína 1 $\alpha$  da heterocromatina. Considerou-se ainda relevante analisar de que modo a fase do ciclo celular



em que a droga é aplicada pode relacionar-se com a quantidade de lesões que surgem no DNA após o tratamento.

No geral, viu-se que a depleção de BRCA1 provoca um aumento no número de células senescentes após o tratamento com Etoposido e Doxorubicina tendo isto sido verificado tanto em condições clonogénicas como em crescimento em massa (*mass growth*). A avaliação da instabilidade genómica através da análise da distribuição de diferentes graus de ploidia demonstrou que a depleção de BRCA1 causa um aumento no número de células com um conteúdo de DNA superior a 4N (conteúdo DNA na fase G2) sendo este aumento mais evidente após o tratamento com Doxorubicina. Em relação à expressão de proteínas associadas à heterocromatina verifica-se concomitantemente uma diminuição da trimetilação da histona H3 no segundo e terceiro dia após o tratamento com Etoposido e um aumento da proteína 1 $\alpha$  da heterocromatina no segundo e terceiro dia ou apenas no segundo dia dependendo do tempo de exposição ao fármaco. No que diz respeito à análise da quantidade de lesões no DNA após o tratamento com Etoposido em diferentes fases do ciclo celular observou-se que existia uma grande variabilidade no número de lesões dentro de cada uma das fases, isto é, para cada fase observam-se células com elevado e com baixo número de lesões. Este resultado, apesar de evidente para os núcleos analisados, necessitará de uma maior amostragem de modo a poder concluir-se com elevado grau de confiança que a quantidade de lesões no DNA é independente da fase do ciclo em que a célula se encontra quando sujeita ao Etoposido.

Em suma, o estudo da resposta a lesões no DNA mediadas por TOP2 possui grande relevância em termos clínicos, uma vez que esta enzima se tornou um dos principais alvos de várias terapias anti-tumorais. O facto da resposta a lesões no DNA poder conduzir não só à apoptose como também à senescência, e de este último fenómeno ser muitas vezes encarado como indesejável no tratamento do cancro, levanta sérias questões sobre até que ponto será vantajosa a indução da senescência mediada por drogas anti-TOP2. Caso se venha a verificar que esta mesma indução durante o tratamento do tumor se correlaciona com um pior prognóstico a longo prazo, quaisquer factores, tais como a análise do estado de BRCA1, que permitam prever este destino celular poderão ser decisivos na escolha de esquemas terapêuticos mais eficazes.

## VIII. Keywords:

DNA topoisomerases

BRCA1

Senescence

DNA damage response

Genomic instability

## **IX. Palavras-chave:**

DNA topoisomerasas

BRCA1

Senescência

Resposta a lesões no DNA

Instabilidade genômica

## I) Introduction:

The topological state of DNA in both prokaryotic and eukaryotic cells is monitored by a special family of enzymes known as DNA topoisomerases [1]. The extended double helix structure of DNA raises several obstacles to key cellular events such as DNA replication, repair, transcription and recombination and this implies the presence of topoisomerases to assure cell viability. These enzymes can be classified into two highly conserved classes, type I and type II [2] [3]. While type I class enzymes catalyse the passage of one strand of the DNA helix through a transient nick in the complementary strand and do not require a high energy cofactor for catalysis, type II class enzymes catalyse the passage of one intact DNA double helix through a transient DNA double strand break which requires the hydrolysis of ATP [2]. Given this distinct mechanism of action type I enzymes are mainly involved in the relaxation of supercoiled DNA whereas type II enzymes can resolve knots, entanglements and catenations [3] (Fig. 1, Annex).

Type II topoisomerases have a three-domain structure viz an ATPase N-terminal region, a DNA binding/cleavage core and a C-terminal tail important for nuclear targeting and interactions with other proteins [4] [5]. Moreover, they are expressed in vertebrates as two closely related but distinct isoforms designated  $\alpha$  (MW= 170 kDa) and  $\beta$  (MW= 180 kDa) which are encoded by separate genes [6] [7] [8]. Dimerisation of these enzymes is a prerequisite for their function and both homo and heterodimers can occur although only the homodimers are active [8] [9]. As for the expression patterns and physiological functions there are several differences between these enzymes namely the up-regulation of the  $\alpha$ -isoform during cell proliferation and its tight association with mitotic chromosomes. In contrast, the  $\beta$ -isoform has an expression pattern that is independent of cell proliferative status and dissociates from chromosomes during mitosis [6] [8] [10]. Additionally, it is known that cells can survive without the  $\beta$ -isoform but not without the  $\alpha$ -isoform since only the latter participates in DNA replication, removing the catenations left on DNA after this process [6].

The relevance of DNA topoisomerases goes well beyond their essential cellular functions; in fact they are the targets for a number of anticancer drugs currently in clinical use [2] [6] namely etoposide (VP-16) and doxorubicin which target primarily topoisomerase II $\alpha$  (TOP2A) [8] but also camptothecin and irinotecan which will target topoisomerase I (TOP1) [11]. All these compounds will promote the stabilization of a reversible reaction intermediate termed the "cleavable complex" which is a normal intermediate in the catalytic cycle of these enzymes (fig. 1, Annex) [12]. This stabilization will change the kinetics of the reaction and cause the enzyme

to remain covalently bound to the DNA for a longer period of time which allows the conversion of the cleavable-complexes into single or double-strand breaks due to collision with the replication fork (TOP1 inhibitors) or with the transcription machinery (TOP2 poisons) [13] [11]. The way cell cycle progression is affected by these drugs also depends on which is used such that the exposure to TOP2 poisons will influence mostly the progression through G2/M with almost no effect on S-phase progression whereas exposure to TOP1 inhibitors will mainly affect S-phase.

Drugs targeting TOP2 can be divided into two broad classes: poisons, which as mentioned above will stabilize the cleavable complex and generate DNA DSBs and catalytic inhibitors that do not induce DNA DSBs and may act either by locking the DNA-bound enzyme in the closed clamp form or by interfering with TOP2 binding to DNA.

The exposure to TOP2 poisons has multiple cellular effects such as altered gene expression and cell cycle arrest, but probably the most important of them all is the triggering of the DNA damage response (DDR) [11]. Generally, the DDR can be divided into three main steps: the detection of the DNA DSB by sensor proteins, the recruitment of transducer and adaptor proteins to the site of lesion that will amplify and diversify the DNA-damage signal and, finally, the enrolment of downstream mediator/effector proteins that regulate various aspects of cellular function including DNA repair [14] [15]. As a consequence of the DNA damage signalling there is a process of cell cycle arrest, termed the “checkpoint response” which can induce a transient delay in G1, S or G2 phases. With respect to the DDR there is still no unanimous chronological pathway, mainly because it is in fact a network of interacting pathways that will work to execute a response depending on cell cycle stage upon induction of the DNA damage [16].

Regarding the signalling processes activated by the presence of DSBs, it is commonly accepted that they depend on the phosphatidylinositol 3-kinase related kinases (PIKKs) ATM (Ataxia Telangiectasia Mutated) and ATR (Ataxia Telangiectasia and RAD3-related) although the main PIKK responsible for the signalling of DSBs is ATM [17]. Recently it has been demonstrated that ATM activation (by intermolecular *trans*-phosphorylation) can be rapidly triggered by changes in chromatin structure even if those changes are not likely to induce DSBs. In light of this evidence it has been proposed that the initiating event in the DDR is a change in chromatin structure derived from the chromosomal damage [18] [19].

Another early event in the DDR is the phosphorylation of H2A.X on Ser 139 (the X member of the H2A histone family) which can be performed either by ATM or by DNA-dependent protein kinase (DNA-PK) [17] [20] [21]. This H2A.X phosphorylation, termed  $\gamma$ -H2A.X,

propagates over megabase-pair regions away from the DSB in both directions - H2A.X foci and is required to either the recruitment or stable retention of mediator proteins such as mediator of DNA damage checkpoint 1 (MDC1), breast-cancer associated protein 1 (BRCA1), p53 binding protein 1 (53BP1) and the MRN (Mre11/Rad50/Nbs1) complex [17] [21]. This latter complex has also been referred to as a candidate sensor for it binds both to ATM and DNA [22] (Fig. 2, Annex).

Activated ATM phosphorylates numerous key proteins namely MDC1, BRCA1, 53BP1 and FANCD2 [23] and, in turn, some of those substrates such as BRCA1, 53BP1 and Nbs1 can function either upstream of ATM or downstream of Chk2 depending on the context [23] [24]. Indeed, it has been shown that a subset of ATM as well as ATR-dependent phosphorylation events require BRCA1 namely phosphorylation of p53, Nbs1 and Chk2 [25]. Once the relevant protein have been recruited and assembled at the site of damage these complexes can engage checkpoint activity to halt DNA replication, which is required for proper repair of damaged DNA [26] (Fig. 2, Annex).

As DSB are considered to be, in general, the most cytotoxic of all DNA lesions, there are efficient and multi-potent mechanisms to repair them, namely the nonhomologous end joining (NHEJ) and homologous recombination (HR) pathways [27] [28]. The nonhomologous end joining pathway (NHEJ), mediated by the DNA-PK complex, functions throughout the cell cycle and is the predominant DSB repair mechanism in the G1 phase [20]. Repair via the homologous recombination pathway (HR) takes place in late S-G2 phase and involves the generation of a single-stranded DNA region to which RPA proteins bind. DSBs which originate from replication fork collapse are also repaired primarily by HR since the fork collapse produces a one-ended DSB (DSE) [20] [29] (Fig. 3, Annex).

Early acting proteins that influence both repair pathways may control the choice of repair pathway [29]. Once a commitment has been made towards one of the repair pathways, specific proteins involved in that pathway will drive the reaction to HR or NHEJ products (fig. 3). It is possible that BRCA1, one of the key players involved in the cellular response to DSBs [14] [28] [30] [31] [32] and which functions in both DSB repair pathways, [33], regulates also the pathway choice although the precise mechanism for this is currently unknown. One hypothesis relies on the evidence that BRCA1 negatively regulates MRN-mediated end processing and thus may suppress the endo- and exonuclease activity of Mre11 allowing for an enhancement in NHEJ accuracy while, at the same time, can interact with BRCA2 which is a critical mediator of the Rad51 strand transferase (step of the HR pathway) [29].

Defects in any of these pathways will cause genome instability and promote tumorigenesis [30] [34] (Fig. 4, Annex). In fact, whenever a break goes unfixed the consequences can be disastrous ranging from gene rearrangements to chromosomal breakdown.

For this reason, the engagement of the DDR can lead either to apoptotic or senescent outcomes in order to block neoplastic progression. Indeed, it has already been shown that senescent human fibroblasts display molecular markers characteristic of cells with DSBs such as  $\gamma$ H2AX foci, 53BP1 and MDC1 [35] and this evidence strengthens the causal relation between DNA damage and senescence (Fig. 5). Senescence is described as a state of permanent cell cycle arrest in which the cell undergoes several distinct biochemical and morphological changes [36] and yet remains metabolically active. Senescent cells show a flat and enlarged morphology and are resistant to apoptosis though the precise mechanism for this feature is unknown [35] [37].

One of the specific markers related to the senescent outcome is senescence-associated  $\beta$ -galactosidase (SA- $\beta$ gal) which is detectable by histochemical staining. In addition, some senescent cells display senescence-associated heterochromatin foci (SAHFs) in euchromatic DNA which are detected by the preferential binding of DNA dyes such as 4',6-diamidino-2-phenylindole (DAPI) as well as by the presence of certain heterochromatin-associated histone modifications (for instance, H3 Lys9 methylation) and proteins [for example, heterochromatin protein-1 (HP1)] [35] [38]. The accumulation of DNA damage is the trigger to all this global changes in nuclear architecture, which also includes a gradual loss of perinuclear and perinucleolar heterochromatin [39]. Although it is believed that senescent cells show chromatin condensation [38], chemical histone deacetylase inhibition (HDCAi) which promotes euchromatin formation, induces senescence [40]. This finding seems to be inconsistent with the role of heterochromatin and SAHFs in both establishing and maintaining the senescent growth arrest. Indeed, it remains clear how senescence can be associated with heterochromatin biogenesis (SAFHs) but also, in other contexts, by activities that promote heterochromatin disruption (HDACi) [35]. Nonetheless, chromatin perturbations have been proposed as another possible cause for senescence. Amongst the numerous functions regulated by BRCA1, this protein has also been shown to induce large-scale chromatin decondensation [41] possibly via its interaction with TOP2 [42].

The stimuli that generate a DDR induce senescence chiefly through the p53 pathway (Fig. 5). P21 is a critical transcriptional target of p53 and mediator of p53-dependent

senescence. In spite of this, p21 is also responsible for a transient growth arrest induced by DNA damage and thus what determines whether cells merely arrest or undergo senescence is currently unknown; it is, however, commonly accepted that a sustained p53-p21 signalling is required for cells to undergo senescence. Whatever the case, there is experimental evidence showing that reduction of p53, p21 or DDR proteins prevents the DNA-damage-initiated senescence and can even reverse the senescent growth arrest [35]. The proliferation of these damaged cells can lead to a state of extensive genomic instability and cell death termed crisis or mitotic catastrophe, which acts as a second barrier to malignant transformation.

In spite of all the benefits that the senescent outcome seems to bring to organisms that are at high risk of developing a neoplastic phenotype there is an emerging, though still largely speculative, idea that the DNA-damage-initiated senescence is a two-edge sword [43]. On one hand, senescent cells can modify the microenvironment that surrounds preneoplastic cells and hence stimulate tumorigenesis [43]. On the other hand, it appears that senescence reversal can occur in case cells senesce without complete engagement of the pRB pathway and subsequently lose p53 function [35] [44] [45]. In either case, this raises concern to what might be the prognosis when cancer patients are treated with drugs that promote the senescent outcome.

In brief, DNA topoisomerases are fundamentally dualistic in nature, not only they are essential to cell viability but also capable of imposing great harm to the cell genome [2]. This dark side of topoisomerases has proven to be of great value in the development of antineoplastic drugs [2]. That is to say, DNA double-strand breaks are probably the most dangerous type of DNA damage insomuch as little as one DSB can be sufficient to kill a cell or trigger apoptosis [30]. Furthermore, an incorrect joining of broken DNA DSBs may lead not only to loss or amplification of chromosomal material but also to translocations in which chromosomal segments are exchanged [30]. In the end, all these events can lead to tumorigenesis and yet we intend to treat cancer using the same weaponry with which it probably arose. Ultimately, future research on this complex network of proteins that function to repair DSBs can unravel some new pathways to develop more effective strategies in cancer therapy as well as help to predict how individual cancer's will respond to existing therapies based on the genotyping and phenotyping of their DNA damage response pathways [29] [30].



## **II) Objectives:**

Drugs that poison DNA topoisomerases and related compounds (inhibitors) have been mainstays in cancer therapy since the 1960s although it was not until 1971 that Wang discovered the first DNA topoisomerase. Actually, these drugs were among the earliest ones to be used in medical oncology and they have become central components of both primary and adjuvant chemotherapy regimens in current usage. In light of this fact, there is a mounting concern on which cellular effects may emerge from exposure to these drugs. Here, we have partially addressed some of the issues raised by these concerns. To do so, we have:

1. Investigated the role of BRCA1 in the cellular senescent outcome after treatment with TOP2 and TOP1 poisons. BRCA1 was chosen due to its key involvement in the DNA damage response and the resulting connection with increased genomic instability, and also to its known involvement in tumorigenesis in humans.
2. Examined how the BRCA1 background interferes with cell cycle distribution and whether it influences or not the cellular DNA content after exposure to both TOP1 and TOP2 drugs.
3. Scrutinized how the cell cycle phase in which cells were exposed to TOP2 poisons influences the amount of  $\gamma$ H2AX foci harbouring DNA lesions (DSBs). It is common knowledge that cancer cells proliferate more than normal cells. Moreover, if a certain cell cycle phase is longer when compared to others, the chance of catching the cells in that particular phase upon drug exposure is higher and so it becomes interesting to know if the effects, with respect to number of lesions, depend on the cell cycle phase.
4. Analysed the status of some heterochromatin markers, in order to assess whether these can be utilized as markers of "pre-senescent" nuclei.

Together, the results to be obtained are expected to clarify the role of TOP2-mediated DNA lesions in genomic instability and in the induction of senescence, and to what extent BRCA1 could act as a modifier of these cellular outcomes.

### **III) Materials and Methods:**

#### **i) Cell culture:**

HCT116 cell lines [HCT116 wt [American Type Culture Collection (ATCC), Rockville, MD], HCT116 p53 K.O. and HCT116 p21 K.O. kindly provided by Dr. Bert Vogelstein] were grown in a 37°C incubator with 5% CO<sub>2</sub> in McCoy's (Gibco BRL) supplemented with L-glutamine (1,5 mM), antibiotics (penicillin and streptomycin) and 10% of fetal bovine serum (FBS). Human embryonic kidney 293T/17 cell line (ATCC) was grown in Dulbecco's Modification to Eagle's Medium (DMEM).

#### **ii) Drugs, chemicals and antibodies:**

Etoposide (VP-16), 4, 6- diamidino-2-phenylindole (DAPI), and 5-bromo-2'-deoxyuridine (BrdU) were purchased from Sigma-Aldrich; Doxorubicin Hydrochloride was from Calbiochem (USA) and Irinotecan was from Pfizer (CAMPTOSAR 20 mg/mL, D5G300). The antibodies used for immunostaining were as follows: mouse monoclonal anti-phospho-Histone H2AX (Ser139) clone JBW301 (Upstate); rabbit polyclonal antibodies against Histone H4, Histone H4 (tri methyl K20), Histone H3 (tri methyl K9) were purchased from Abcam (USA); mouse monoclonal anti Histone H3 (Abcam); sheep polyclonal against BrdU (Bioss International). Alexa488, FITC and Texas red-conjugated affinity purified secondary antibodies were purchased from Jackson ImmunoResearch Laboratories (West Grove, PA).

The antibodies used for western blotting include: mouse monoclonal anti-Bra1 (Calbiochem), mouse monoclonal anti- $\beta$ actin (Sigma-Aldrich); also the rabbit polyclonal antibodies against Histone H4, Histone H4 (tri methyl K20), Histone H3 (tri methyl K9) and the mouse monoclonal anti Histone H3 (Abcam).

MTT reagent ((3-(4, 5-dimethylthiazolyl-2)-2, 5-diphenyltetrazolium bromide)) was purchased from Calbiochem.

Transfection material includes: pCMV-dR8.91 (TRC); VSV-G (TRC); TransIT-LT1 transfection reagent (MirusBio); OPTI-MEM serum-free media (Invitrogen); DMEM (Dulbecco's Modification to Eagle's Medium; Mediatech); iFBS (heat-inactivated FBS; HyClone); Polybrene (Hexadimethrine bromide; Sigma) and Puromycin Dihydrochloride (Sigma).

Histochemical staining of  $\beta$ -galactosidase activity was performed using the Senescence cells histochemical staining kit (purchased from Sigma-Aldrich) as per the manufacturer instructions.

### **iii) Transfection of small hairpin RNA**

The small hairpin RNAs used were obtained from The RNAi Consortium (TCR). These include: BRCA1.I, BRCA1.II, BRCA1.III, BRCA1.IV and SCRAMBLE. The preparation of transfection-quality plasmid DNA was as described in [46]. Lentiviral production and infection were as detailed in TCR Lentivirus production protocol Part 2 (18 Jan 2007) and in TCR Lentivirus infection protocol Part 1 (9 Feb 2009). In brief, the most relevant steps in the transfection process were as follows:

- Lentiviral production: 293T packaging cell line was seeded at  $2.2 \times 10^5$  cell/mL in low-antibiotic growth media [DMEM + 10% iFBS (heat-inactivated FBS) + 0.1x Pen/Strep] in a 96 well-plate. After approximately 24 hours cells were transfected with the transfection mix containing packaging and VSV-G envelope plasmids, the hairpin-pLKO.1 of interest and the TransIT-LT1 transfection reagent (diluted in OPTI-MEM). After 18-20 hours the medium was changed and replaced with high serum growth media. Cells were incubated for 24 hours and the medium containing the viral pool was harvested and stored at  $-80^{\circ}\text{C}$ .

- Lentiviral infection: HCT116 cell line/s was/were seeded in a 24-well plate. The media was replaced for fresh media containing polybrene and then the viruses were added. Cells were spun at 2250 rpm in plate for 90 min at  $37^{\circ}\text{C}$ . Media was changed immediately after the spin infection. After 24 hours puromycin (1mg/mL) was added to each well. The puromycin selection lasted for 4 days post-transfection.

### **iv) Western blotting**

Total cell extracts were prepared by adding Laemmli 2X buffer (125 mM Tris pH 6.8, 4% SDS, 20% glycerol, 0.004% bromophenol blue, 10 % 2-mercaptoethanol). Cells were scraped from the dish, transferred to an eppendorf and boiled for 10 min at  $95^{\circ}\text{C}$ . To analyse the knock-down status of BRCA1, an aliquot of cell suspension was collected to an eppendorf, centrifuged at 3000 rpm for 5 min at  $4^{\circ}\text{C}$ , washed with PBS, resuspended in 2X concentrated electrophoresis sample buffer and finally boiled for 10 min at  $95^{\circ}\text{C}$ . The protein extracts were kept at  $-20^{\circ}\text{C}$ . To reduce viscosity cells were treated with benzonase ( ) for 20 min at room temperature previously to loading and running the gel.

Detection of high molecular weight proteins was done using a 7% polyacrylamide gel while detection of lower molecular weight species was done using a 14% polyacrylamide gel.

Coomassie staining was used to visualize the low molecular weight proteins. The 14% gels were incubated with Coomassie Brilliant Blue solution for 1 hour with mild agitation. For

destaining, gels were incubated with Coomassie Destain solution with mild agitation until the excess dye had been removed.

For wet transfer of proteins to nitrocellulose membranes conditions were 90 min at 250 mA to high molecular weight proteins and 45 min at 80 mA to small molecular weight proteins. A reversible Ponceau Red staining was used to check for success of transfer.

The membranes were blocked using a 5% non-fat skimmed milk solution in PBS 1x. It was incubated for 1 hour at room temperature under agitation.

The incubation time with primary and secondary antibodies was 2 hours, and the membrane was washed several times with PBS 1x after each incubation time.

An ECL detection kit was used to detect HRP-conjugated antibodies.

#### **v) Immunolabeling procedures:**

Cells growing on coverslips were fixed either in PHT [Paraformaldehyde (PFA) 7.4%, HPEM 2x buffer and Triton X-100] for 10 min at room temperature with mild agitation or in PFA 1% for 1 min followed by Methanol at -20°C for 10 min. Cells were kept in PBS-Tx (PBS 1x buffer and Triton X-100 0.05%) at 4°C until immunostaining. Primary and secondary dilutions as well as washes during the immunostaining procedure were done in PBS-Tx. Coverslips were incubated for 1 hour in a 37°C humid chamber with both the primary and secondary antibodies. Coverslips were washed several times after the two incubations. For post-staining fixation cells were left in FA 2% in PBS for 10 min then washed several times and mounted in Vectashield + 4, 6-diamidino-2-phenylindole (DAPI). In double-labelling experiments with a sheep polyclonal anti-BrdU antibody and a mouse monoclonal specific for H2AX, H2AX detection preceded that of BrdU and the incubation time with both the primary and secondary antibodies was twice the usual incubation time. After H2AX immunostaining cells were subjected to 4N HCl for 10 min, in dark, in order to accomplish DNA depurination. Acid neutralization was achieved by leaving the coverslips in PBS-Tx + Tris 0.1M pH 8.0, in the dark for at least 1 hour. BrdU staining followed as described after these two key steps. For DAPI quantifications cells were left in DAPI (1mg/ml) in PBS-Tx for 5 min and then mounted in Vectashield medium.

#### **vi) The MTT assay**

Cells were plated in 96-well plates to test different concentrations of Irinotecan and Doxorubicin. Following each drug exposure the medium was replaced; after 24 hours the MTT solution was added to a final concentration of 1mg/mL in each well. Plates were left for 2 hours at 37°C with 5% CO<sub>2</sub>. The medium was then removed and a DMSO + glycine buffer (pH=10.5) solution was added. Plates were read at 570 nm with Tecan i-Control 1.4.5.0 software.

#### **vii) Clonogenic assay**

Cells were seeded and treated with Irinotecan, Doxorubicin or Etoposide when a suitable cellular density was reached (approximately 60% confluency). After drug exposure, cells were incubated with fresh drug-free medium and allowed to recover for 1 hour at 37°C with 5% CO<sub>2</sub>. The appropriate number of cells was plated in 10 cm Petri-dishes in order to allow the formation of colonies within 1 week. After this time cells were fixed with 2% FA in PBS, 1 min followed by Methanol, 10 min at room temperature. Then, cells were hydrated in distilled water for 1 min, stained with haematoxylin for 5 min, washed two times with water and finally dehydrated with Ethanol [70% (1 min), 95% (1 min) and 100% (1 min)].

#### **viii) Flow cytometry assay:**

For DNA content analysis, cells were plated in 6-well plates and treated with different drugs according to the specific experimental procedures. Cells were then fixed in 70% ethanol (at least for 4 hours) at 4°C and stained with Propidium Iodide (PI) approximately two hours before flow cytometry acquisition.

#### **ix) Senescence-associated $\beta$ -galactosidase assay:**

Cells growing exponentially were treated with Etoposide and the Senescence-associated  $\beta$ -galactosidase (SA  $\beta$ -gal) staining was done following the Senescence Cells Histochemical Staining Kit protocol using Nuclear Fast Red as counterstaining.

## IV) RESULTS:

### i) Cell line characterization:

In order to accomplish our objectives we had to first determine the doubling time and the duration of the cell cycle phases of the cell lines used in this project viz HCT116 wild type for p53 and p21 (WT), HCT116 p53 knock-out (K.O.) and HCT116 p21 knock-out (K.O.). To do so, we generated their respective growth curve, as well as, for HCT116 WT cell line a diagram of labelled mitoses. From each growth curve, we determined the doubling time of the respective cell line. For this reason we could establish the following doubling times:

- HCT116 WT (p53 +/+ and p21 +/+): 15,16 hours (15h and 10min), (Fig. 6)
- HCT116 p53 K.O.: 16,61 hours (16h and 37min), (Fig. 7)
- HCT116 p21 K.O.: 19,77 hours (19h and 46min), (Fig. 8)

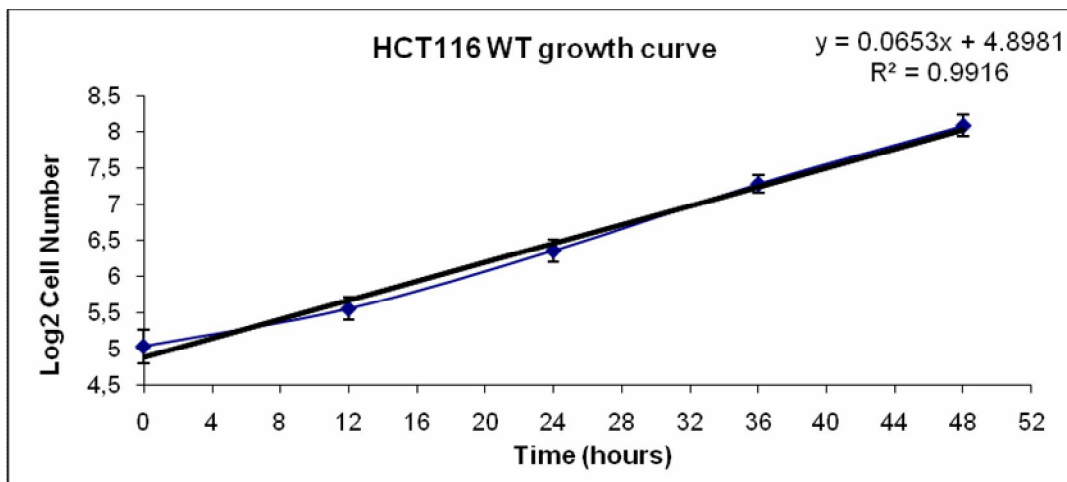


Figure 6: HCT116 WT growth curve. HCT116 WT cells growing exponentially were plated and counted in a haemocytometer every 12 hours. Results were plotted on a log-linear scale. The population-doubling time was determined using the linear regression equation displayed on the graph. HCT116 WT cell line has a doubling time of 15h and 10 min.

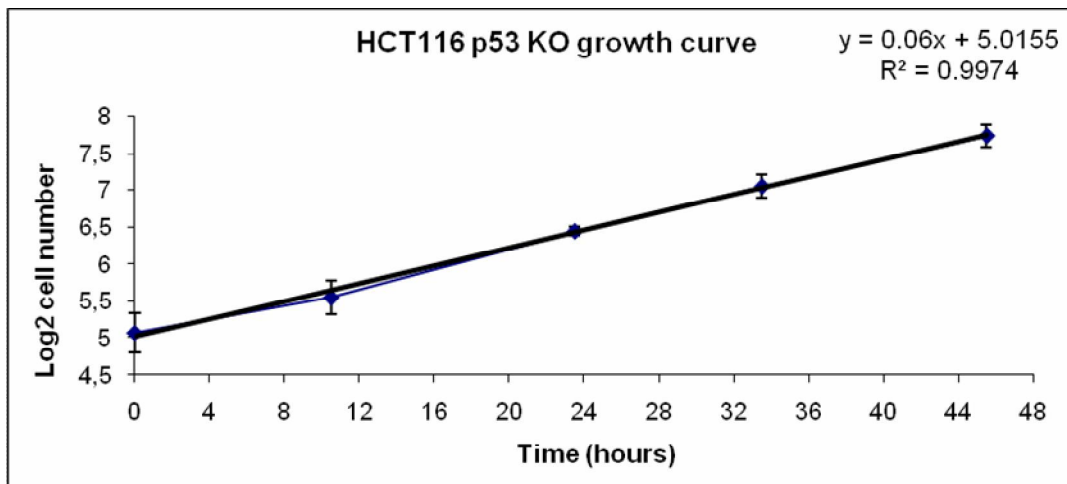


Figure 7: HCT116 p53 K.O. growth curve. HCT116 p53 K.O. cells growing exponentially were plated and counted in a haemocytometer every 11 hours. Results were plotted on a log-linear scale. The population-doubling time was determined using the linear regression equation displayed on the graph. HCT116 p53 K.O. cell line has a doubling time of 16h and 37 min.

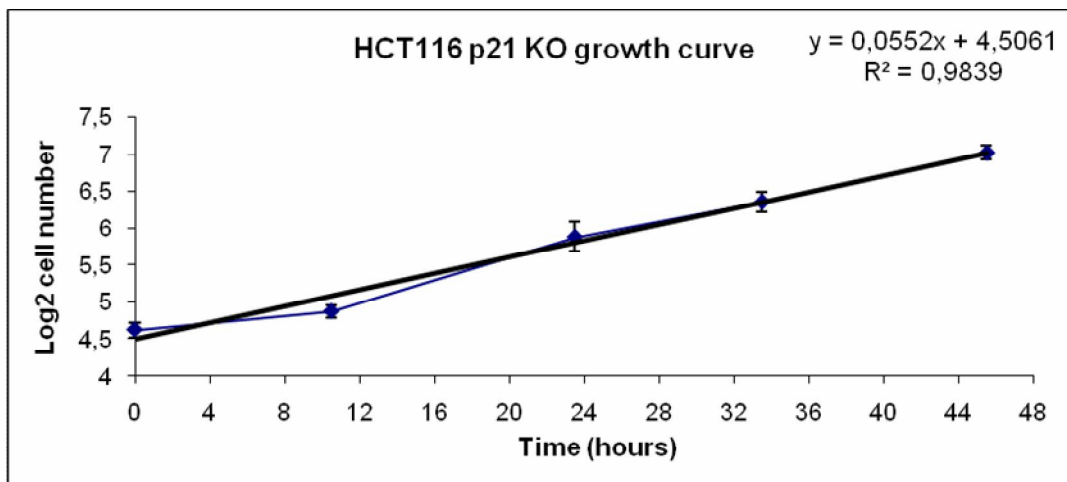


Figure 8: HCT116 p21 KO growth curve. HCT116 p21 K.O. cells growing exponentially were plated and counted in a haemocytometer every 11 hours. Results were plotted on a log-linear scale. The population doubling time was determined using the linear regression equation displayed on the graph. HCT116 p21 K.O. cell line has a doubling time of 19h and 46 min.

In what concerns the diagram of labelled mitosis it is convenient to explain in a little more detail the rationale behind the method. Labelled mitosis is a method of relating measurements on single cells to the cell cycle and consists on scoring labelled mitosis in samples collected at successive time points. In essence, we give a pulse of BrdU, which is a thymidine analogue that will only be incorporated by replicating cells [47] [48]. Afterwards we start sampling the cells at defined intervals and from each one of those intervals we count the number of mitoses that are

BrdU-labelled under the microscope and determine the percentage of labelled mitoses (Fig. 9, Annex and Tab. 1). The principle behind this approach is simple since labelled mitoses can only emerge after cells that were transversing S-phase have progressed through G2 phase. The labelled mitoses do not come all at once since cells were at different S-phase stages in the beginning (Diag. 1, Annex). From the point where approximately all mitoses are labelled (which implies that all cells from the different S phase stages reached mitosis) we start to see a trough as cells that were initially in G1 come to the end of their cycle (Diag. 1, Annex). The duration of the different phases of the cell cycle is conventionally determined using the 50% points.

Therefore, the time between the start of the experiment and the 50% point in the ascending curve will correspond to the duration of G2 phase plus half the mitosis duration, the time between the 50% points in the ascending and in the descending portions of the curve correspond to S phase duration. The duration of G1 will be determined by subtracting from the total cell cycle time (time between two similar points in the curve) the duration of G2, S and M phases. The great advantage of this method is giving the absolute duration of the cell cycle phases although one should be careful not to use synchronous cells in this assay.

Time collection (after BrdU pulse)	Number of mitotic cells	Number of mitotic cells BrdU+	% Mitotic cells BrdU+
2h	250	0	0
3h	250	0	0
4h	256	24	9.37%
5h	252	165	65.47%
6h	250	226	90.40%
7h	253	245	96.80%
8h	250	249	99.60%
9h	257	250	97.27%
10h	250	240	96.50%
11h	250	160	64%
12h	250	87	34.80%

**Table 1:** Percentage of HCT116 WT mitotic BrdU positive (+) cells at each time point. For each time point approximately 250 cells were analyzed and classified as either BrdU positive (+) or BrdU negative (-). The percentage of mitotic cells BrdU positive (+) was determined for each time point.



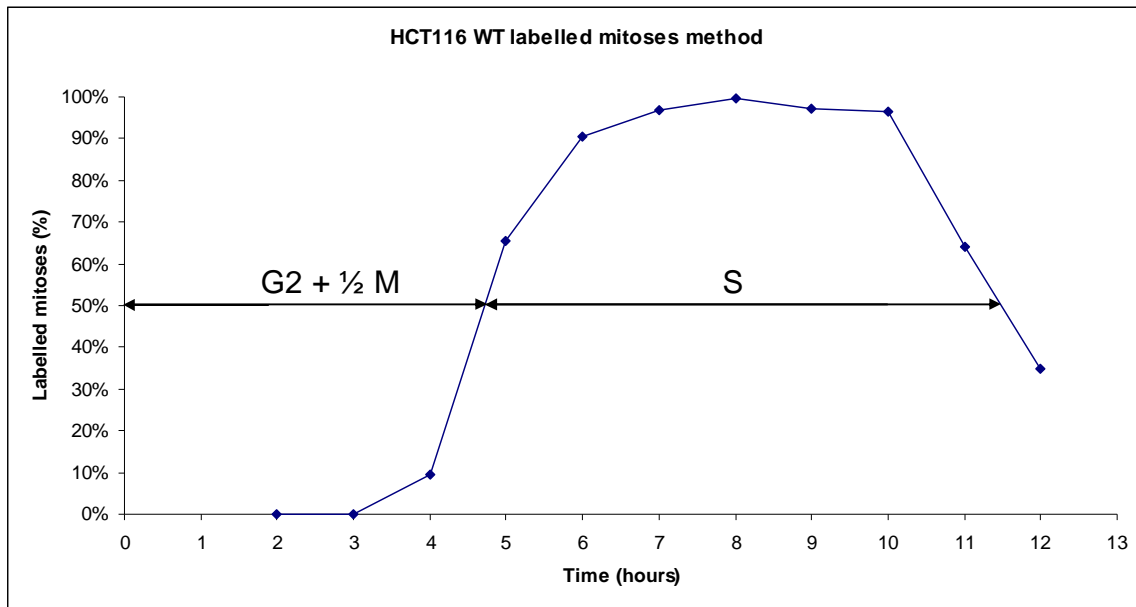


**Figure 10:** HCT116 WT labelled mitosis graph. The percentage of mitotic cells BrdU positive (+) at each time point were plotted in the graph and the 50% points in the ascending and descending portions of the curve were determined.

With respect to the HCT116 WT cell line, we could conclude that the G2 phase duration is 4h (4h 45 min minus 45 min of ½ M), the S-phase duration is 6h and 20 min and the G1 phase duration is 3h (Fig. 10). This last result was obtained resorting to the duplication time calculated from the growth curve of this cell line since the sampling intervals used in our BrdU labelled mitosis experiment did not allow us to reach the end of a complete cell cycle.

Beyond, we could also define the duration of the different S-phase stages given that S-phase BrdU positive cells display replication patterns that can easily be identify and scored to each stage. Using this approach, we were able to come up with the following results (Tab. 2):

Replication Pattern	Number BrdU+ cells	Replication Pattern %	Duration (hours)
1	97	36.7%	2.3
2	67	25.4%	1.6
3	54	20.5%	1.3
4 and 5	46	17.4%	1.1
All	264	100%	6.3

**Table 2:** Absolute duration of each S phase sub-stages in HCT116 WT cell line. For determination of the absolute duration of each S phase sub-stage 264 cells from the 2h time point were classified according to their replication pattern.

The first and second replication patterns are considered Early S-phase stages, the third is considered a Mid S-phase stage and, finally, the fourth and fifth correspond to Late S-phase stages [49].

Characterizing the biological material we intended to use in our project is of great importance when defining our experimental work, and in this case, it proved to be an exceptional tool for other experimental approaches [50]. In addition, it is fundamental to assure the quality of the cell lines in order to perform successful experimentation. This becomes even more relevant given that a growing amount of evidence demonstrates that cell lines at high passage numbers in culture experience modifications in cell morphology as well as in growth rates and protein expression when compared to lower passage cells (e.g., ATCC Technical Bulletin no. 7, 2007).

#### **ii) MTT cytotoxicity assay:**

Cytotoxicity assays are widely used as a powerful tool to measure the effect of a certain drug on cell growth. The basis of the MTT assay consists of exposing cells in exponential growth to a cytotoxic drug (exposure time and drug dosage vary accordingly to the final goal of the experiment); after its removal, cells are allowed to proliferate for two or three doubling times so we can distinguish between cells that are not only viable but also capable of proliferation from cells that although viable cannot proliferate. The number of viable cells is an indirect measure of MTT dye reduction. In essence, MTT is a water-soluble yellow dye that is reduced by viable cells to a purple formazan product insoluble in aqueous solutions. The amount of product will be proportional to the number of viable cells and can be determined spectrophotometrically after its solubilisation [51]. In light of this determination we can also obtain the half maximal inhibitory concentration ( $IC_{50}$ ) which is the drug concentration at which we reduce the population growth by 50%, in vitro. Therefore, we next determined the effect of different concentrations of doxorubicin and irinotecan in the growth of HCT116 WT, HCT116 p53 K.O. and HCT116 p21 K.O. cell lines. Exposure times to irinotecan and doxorubicin were 12 and 4 hours, respectively.

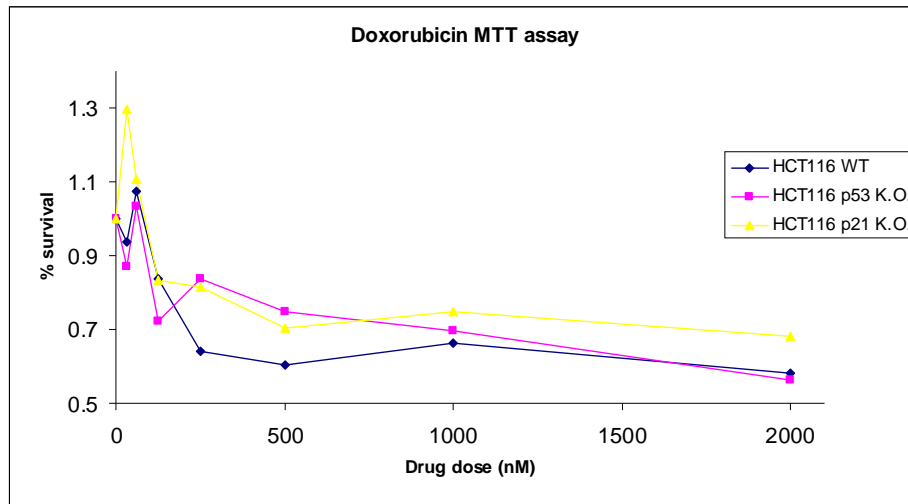


Figure 11: Determination of percentage of survival after doxorubicin treatment. Note that, with 500 nM of doxorubicin, HCT116 WT, HCT116 p53 K.O. and HCT116 p21 K.O. have not yet reached the IC<sub>50</sub>. The percentage of survival with 500 nM of doxorubicin in all three cell lines does not vary significantly.

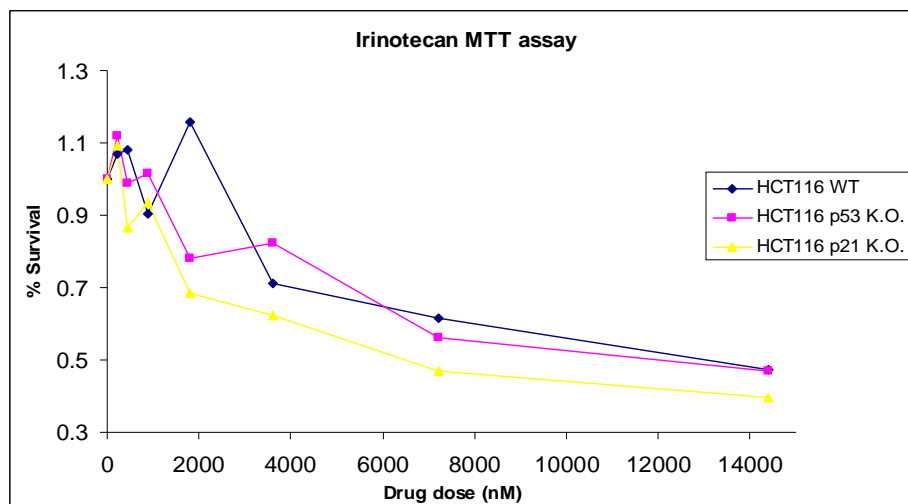


Figure 12: Determination of percentage survival after irinotecan treatment. Note that, with 3600 nM of irinotecan, HCT116 WT, HCT116 p53 K.O. and HCT116 p21 K.O. have an overall survival close to 70%.

Regardless some points in the graphs, which are incongruent with what was expected, the main reason for this assay was assessing the sensitivity of each cell line to each of the two drugs. Therefore, we could retrieve at least two very important hints from the two graphs: firstly, even a staggeringly high dosage of doxorubicin was not enough to reach the IC<sub>50</sub> in any of the cell lines used (Fig. 11) and secondly, only an exaggerated dose of irinotecan seemed sufficient to achieve the IC<sub>50</sub> in all the cell lines (Fig. 12). Nevertheless, it is important to notice that all the three cell lines seem to behave similarly with respect both to the doxorubicin and irinotecan drug

concentrations. Whenever possible we have used clinically relevant dosages of these drugs in the following experiments.

### iii) Clonogenic assay, the gold standard of cell sensitivity assays:

The preceding results are very important and certainly true for a first approach, but to achieve a higher level of accuracy it is very important to corroborate the MTT results with the clonogenic assay. The basic differences between these two assays reside on the fact that in the clonogenic assay, after releasing the cells from the drug they are disaggregated in order to form a single-cell suspension that is then plated at low density. In the end and considering a perfect system, we would be plating single cells trough out the Petri dish and each one of these cells would have the potential to origin a colony in which all cells would be clones of the one seeded. Despite a few variables that cannot be controlled in the assay it is until now regarded as the “gold standard” cellular-sensitivity assay [52]. The following clonogenic experiments were done not only to confirm the MTT results but also to address whether HCT116 WT cells, with or without BRCA1 knock-down (k.d.) termed BRCA1 k.d. and SCRAMB respectively, had a significant difference in sensitivity to Doxorubicin and Etoposide.

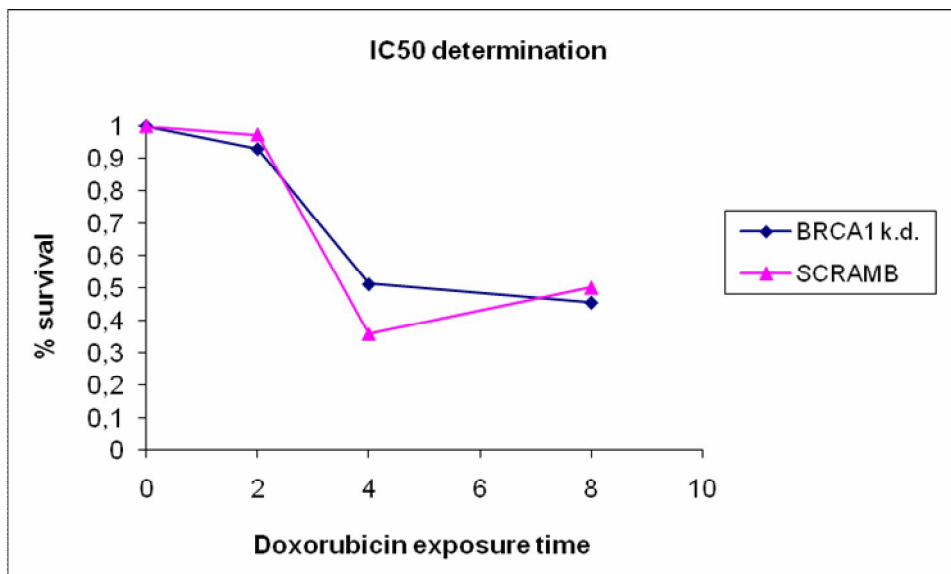


**Figure 13:** Clonogenic survival assay after doxorubicin treatment. HCT116 BRCA1 k.d. and SCRAMB cells were treated with doxorubicin (500nM, 2h, 4h and 8h) and plated in clonogenic conditions. After one week cells were stained with haematoxylin and counted (both single-cells and colonies). IC<sub>50</sub> for doxorubicin was achieved with 4h exposure to the drug. The increase in % survival with 8h exposure compared to 4h exposure in SCRAMB cells might be a technical artifact. Future experiments shall confirm this result.

To determine the IC<sub>50</sub> of etoposide and doxorubicin, HCT116 WT cells were treated within each experimental group to the same concentrations of etoposide (50 µM) or doxorubicin (500 nM) respectively. These concentrations were determined based on the previous MTT assay as well as on other experimental data not shown. The exposure times varied within a range adequate for each drug cytotoxic level.

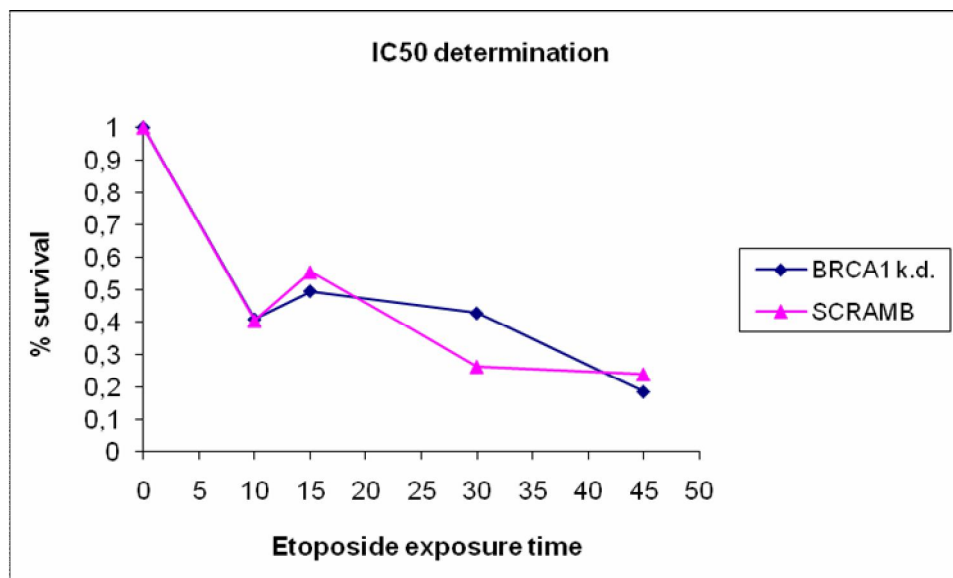


**Figure 14:** Clonogenic survival assay after etoposide treatment. HCT116 BRCA1 k.d. and SCRAMB cells were treated with etoposide (50µM, 10 min, 15 min, 30 min and 45 min) and plated under clonogenic conditions. After one week cells were stained with haematoxylin and counted (both single-cells and colonies). IC<sub>50</sub> for etoposide was achieved with 15 min exposure to the drug. The increase in % survival with 15 min exposure compared to 10 min in both SCRAMB and BRCA1 k.d. cells might be a technical artifact. Future experiments shall confirm this result.

We could observe that for both BRCA1 k.d. and SCRAMB (transfection control) cells, 4 hours exposure to 500 nM of doxorubicin was close to the IC<sub>50</sub> (Fig. 13). In what concerns etoposide, 15 min exposure to 50 µM seemed to be sufficient to reach approximately the IC<sub>50</sub> value (Fig. 14).

Importantly, we could conclude that exposure to 50 µM of etoposide during 15 min had the same effect on the percentage of survival as 500 nM doxorubicin during 4 hours and we also established that the sensitivity of SCRAMB and BRCA1 k.d. cells to drugs is nearly equivalent. These results shall be further validated in future experiments.

#### iv) BRCA1 plays a role in triggering the senescent cellular outcome following exposure to Topoisomerase II poisons:

Just as mentioned in the introduction, BRCA1 plays a major role in the DDR. As a matter of fact, it would not be difficult to hypothesize that decreasing its protein expression would have profound effects on cellular recovery after exposure to TOP2 poisons. In addition, some reports have already correlated the DDR to the senescent outcome. In order to address a potential role for BRCA1 in senescence we did a knock-down (k.d.) of BRCA1 (Fig. 15, Annex 1). Next, we exposed BRCA1 k.d. and SCRAMB (transfection control) cells to TOP2 poison doxorubicin (500 nM, 4h) and TOP1 drug irinotecan (3600 nM, 12h) and evaluated the senescent outcome of these cells by clonogenic assay (Fig. 16, Annex). We have also decided to see whether the BRCA1 k.d. effect on the senescent outcome was dependent on both the p53 and p21 genetic background of the cell lines since it is known that these genes are involved in one of the pathways that leads to senescence.

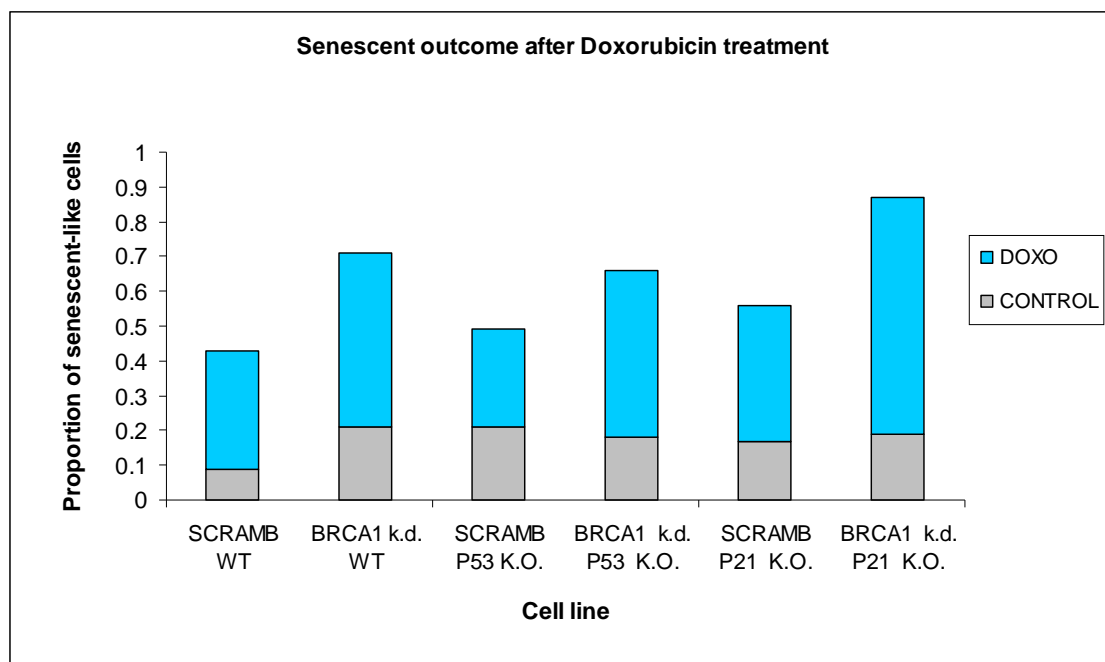


**Figure 17:** Senescent outcome after doxorubicin treatment. SCRAMB and BRCA1 k.d. cells were stained with haematoxylin and classified as either senescent-like or normal looking cells. BRCA1 k.d. cells displayed a significant increase in the proportion of senescent-like cells compared to SCRAMB cells.

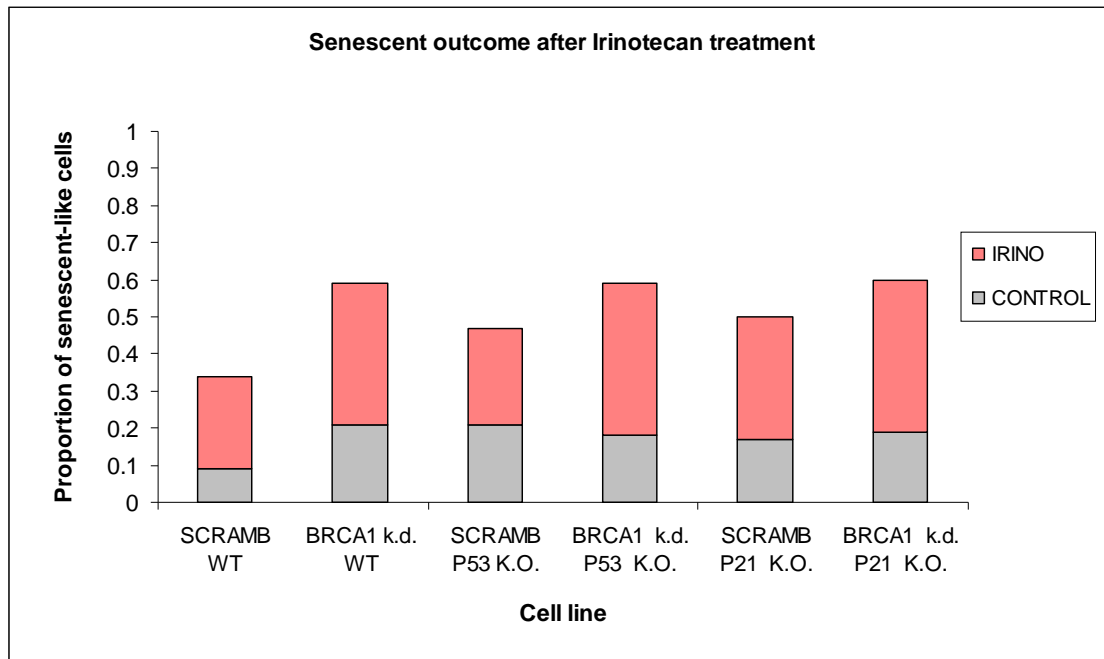


**Figure 18:** Senescent outcome after irinotecan treatment. SCRAMB and BRCA1 k.d. cells were stained with haematoxylin and classified as either senescent-like or normal looking cells. BRCA1 k.d. cells displayed a slight increase in the proportion of senescent-like cells compared to SCRAMB cells.

The results obtained are summarized briefly bellow:

- BRCA1 *k.d.* causes an increase in the number of senescent-like cells after doxorubicin treatment when compared to SCRAMB (17% in HCT116 WT and 21% in HCT116 p53 K.O.). Additionally, this increase seems to be more accentuated in the p21 K.O. cell line (40%), (Fig. 17).
- BRCA1 *k.d.* causes an increase in the number of senescent-like cells following irinotecan treatment. However, this increase is considerably lower compared the increase after doxorubicin exposure (13% in HCT116 WT, 15% in p53 K.O. and 8% in HCT116 p21 K.O.), (Fig. 18).
- Overall, the genetic background of the three cells lines, HCT116 WT, HCT116 p53 K.O. and HCT116 p21 K.O. does not seem to influence by far the senescent outcome.

Etoposide treatment leads to an elevated rate of cell death and so it is very difficult to assess its effect on the senescent outcome by clonogenic assay. Therefore, we used the senescence-associated  $\beta$ -galactosidase (SA- $\beta$ gal) assay given that SA- $\beta$ gal is a commonly accepted marker of senescent cells (Fig. 19, Annex). Following etoposide treatment (50  $\mu$ M, 15 min) it was observed a large increase the senescent outcome in BRCA1 *k.d.* cells but not in

SCRAMB cells (46%), (Fig. 20). The cell counts were different between SCRAMB and BRCA1 samples, 510 and 341 cells respectively but this fact does not alter our conclusion. It even reinforces the significance of our result. Altogether, we could conclude that depletion of BRCA1 causes an increase in senescent-like cells following treatment with etoposide.

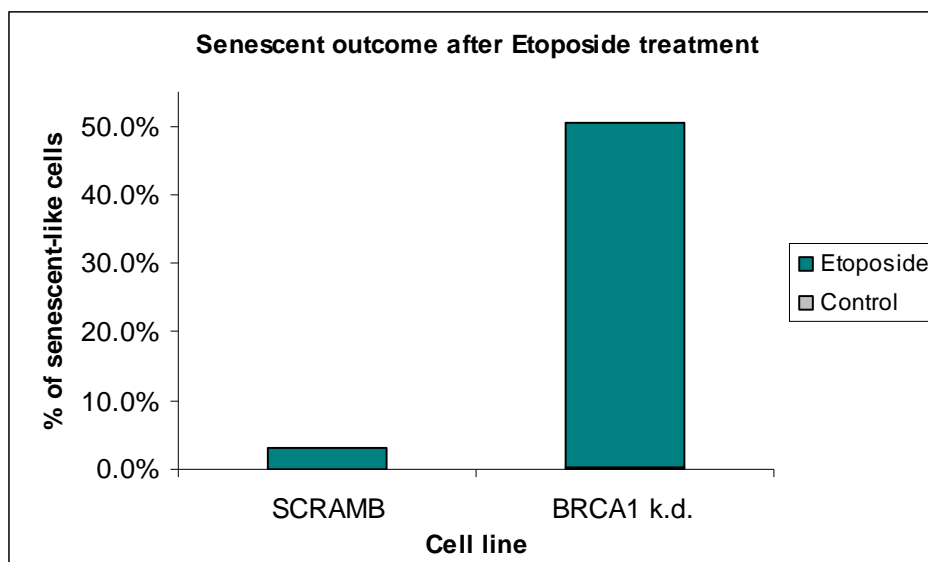


**Figure 20:** Senescent outcome following etoposide treatment (50  $\mu$ M, 15 min). Exponentially growing cells were stained for senescence-associated  $\beta$ -galactosidase and imaged by brightfield microscopy using identical image capture settings. For SCRAMB, 785 cells in the control (no treatment) group and 510 in the etoposide group were analysed. For BRCA1 k.d., 978 cells in the control group and 341 in the etoposide group were analysed. BRCA1 k.d. cells displayed an increase of 46% in the senescent outcome compared to SCRAMB cells.

## v) Time course analysis of the effect of TOP2 and TOP1 drugs in cell cycle distribution and cellular DNA content:

### a) Etoposide induces a subtle increase in the cellular DNA content:

Type II DNA topoisomerases are known for their role in detangling daughter chromatids at anaphase of mitosis [53]. In response to TOP2 poisons p53 signalling can initiate cell cycle arrest, cellular senescence or apoptosis to eliminate genomically unstable cells and suppress tumorigenesis. Therefore, one can hypothesize that inhibiting the activity of these enzymes may lead to an increase in cellular ploidy. In fact, it has been observed in several reports that the use of TOP2 catalytic inhibitors results in the formation of polyploid nuclei as a consequence of chromosome segregation failure [33] [54]. With respect to TOP2 poisons this assumption is far more difficult to retrieve since they lead not only to cytotoxic effects but also to induction of DNA damage with subsequent G2 delay [54] [55]. Until date, the influence of TOP2 poisons in the formation of polyploid nuclei has been assessed, employing a continuous exposure to the drug.



To address this issue from a different perspective, cells were treated with a short etoposide pulse, which results in acute instead of chronic cellular exposure to the drug (Diag. 2). With this regimen, cells were allowed to recover the catalytic functions of TOP2 [which can be demonstrated by the Differential Retention of Topoisomerase II (DRT) assay that measures the amount of catalytically active enzyme] and for that reason, whatever effect observed in cellular ploidy cannot derive from lack of TOP2 activity.

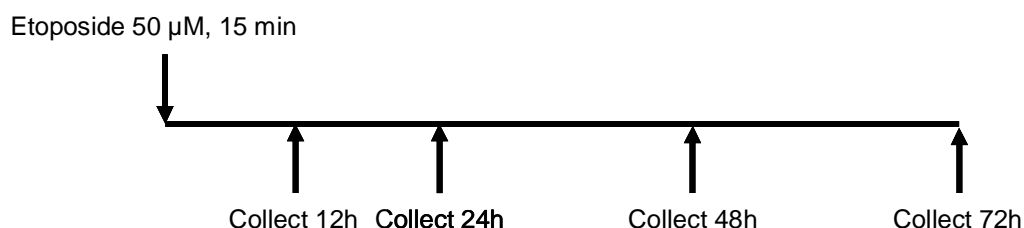


**Diagram 2:** Experimental plan details. Cells growing exponentially were exposed to a short pulse of etoposide (50μM, 15 min) and collected at defined time points (12h, 24h, 48h and 72h after the pulse) for microscopy analysis.

Each sample was stained with DAPI, which allowed us to look and analyse specifically the population of cells with high cellular DNA content. In what concerns the analysis of the samples, this was done using the Image J software with which we were able to select each nuclei individually, obtain the area, and mean intensity (pixels). With these two parameters, the total DAPI intensity was calculated, which corresponds to the total DNA content of the nuclei. Next, the total DAPI intensity values obtained from the samples were split in several classes because in each time point, there was a mixture of nuclei with different DNA contents and we wanted to analyse their respective distribution among the different classes. In the end, we could clearly distinguish a shift in the nuclei distribution between the control and the 72h timepoint (Fig. 21). In addition, this change occurred gradually along the other time points. The nuclei from the control sample were almost all within a short range of low total DAPI intensities while the nuclei from the 72h timepoint were spread along a wide range of high total DAPI intensities. Moreover, we have observed that larger nuclear sizes are usually associated with higher cellular DNA content. Altogether, we can conclude that cells exposed to etoposide for a short period of time (15 min) display an increase in their DNA content. This result shall be confirmed with additional measurements.

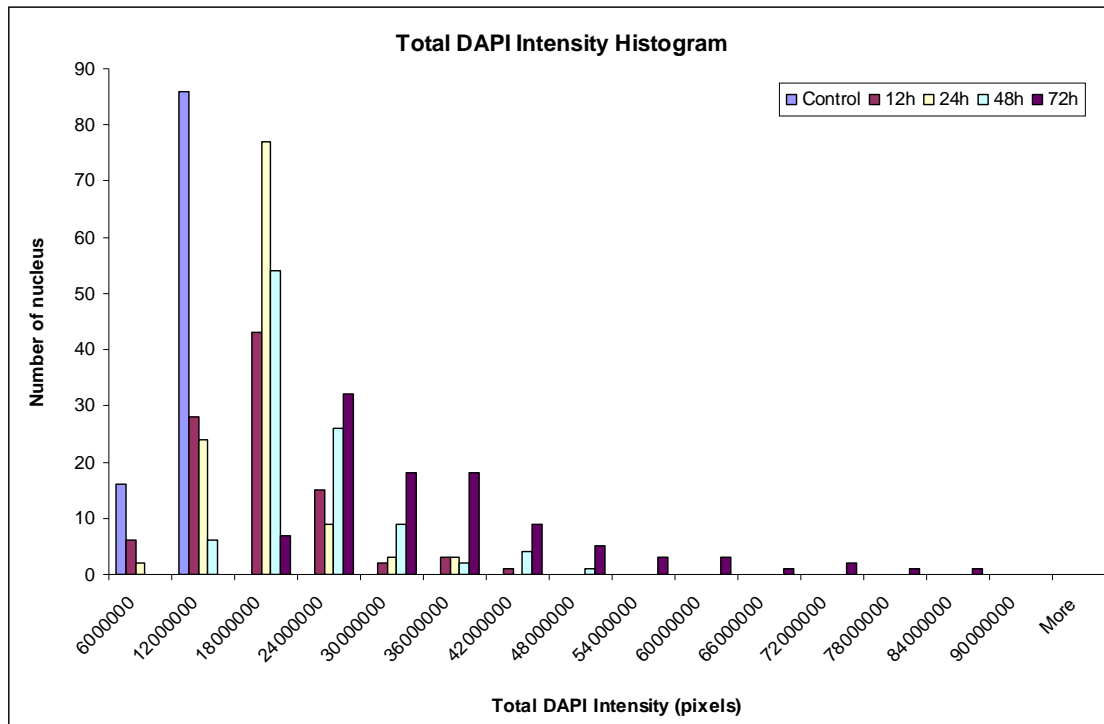


**Figure 21:** Total DAPI Intensity Histogram. Cells were grown in coverslips and treated with etoposide (50 $\mu$ M, 15 min). DNA was stained with DAPI;  $\geq 100$  nuclei per experimental group were analysed and distributed according to the total DAPI intensity range. Note that 72h after exposure to etoposide roughly all nuclei were distributed across a wide range of high total DAPI intensities.

### **b) BRCA1 knock-down increases the number of cells with high DNA contents after exposure to Doxorubicin**

We have observed in the previous results that etoposide exposure leads to an increase in the cellular DNA content via genomic instability. Moreover, several reports show that BRCA1 is involved in maintenance of genomic integrity. Therefore we proposed to determine whether the knock-down of a BRCA1 leads to an increase in genomic instability via an increase in the cellular DNA content (ploidy) after exposure to topoisomerase drugs. Due to experimental limitations we did not collect 72h and 12h time points.

One striking feature we could immediately observed in the controls was a higher number of BRCA1 k.d. cells with higher DNA contents (Mean % > G2) compared to the SCRAMB group (transfection controls). Still, there was not much difference between BRCA1 k.d. and SCRAMB in terms of the distribution of cells within the different cell cycle phases (Fig. 22).

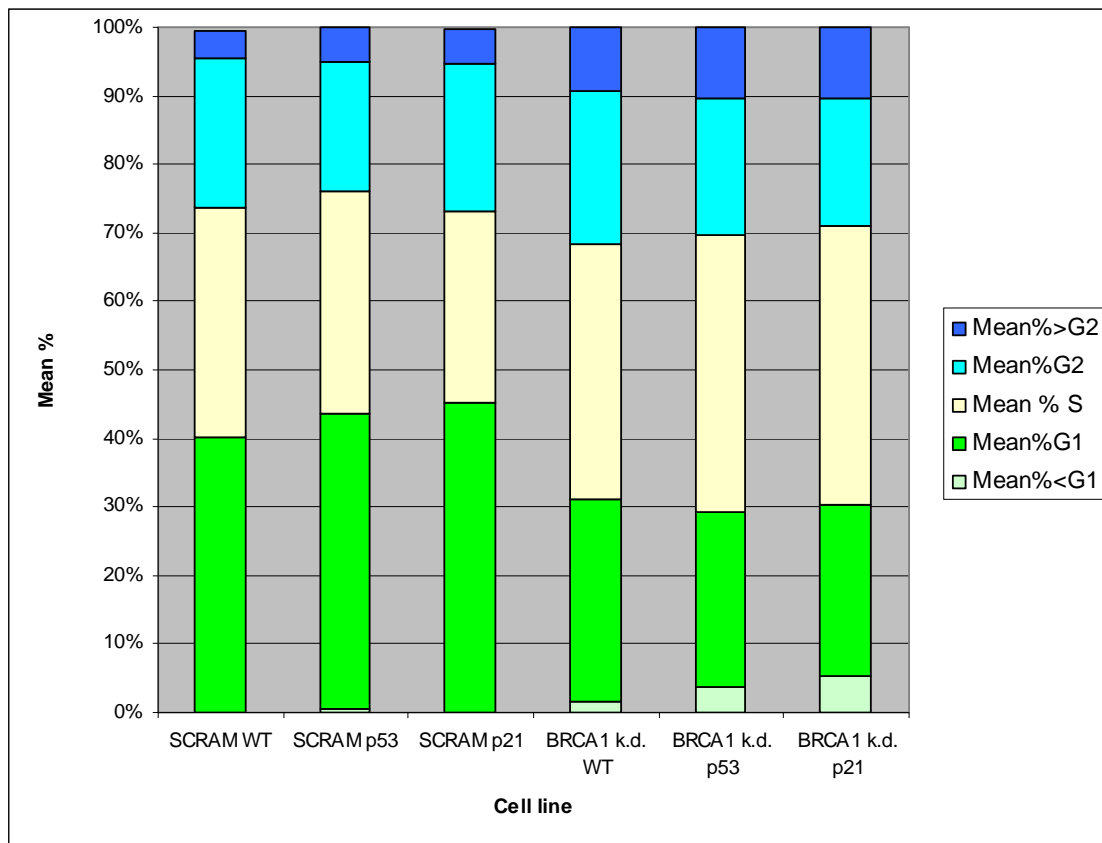


**Figure 22:** Flow cytometry analysis of cell cycle distribution in the controls. . HCT116 WT, p53 K.O. and p21 K.O cell lines with BRCA1 k.d. were designated (BRCA1 k.d. WT, BRCA1 k.d. p53 and BRCA1 k.d. p21 respectively). HCT116 WT, p53 K.O. and p21 K.O cell lines without BRCA1 k.d. were designated (SCRAMB WT, SCRAMB p53 and SCRAMB p21 respectively). Cells growing exponentially were treated with DMSO for 4h, allowed to recover for 1h and then fixed with ethanol 70%. Cells were stained with propidium iodide at least 2h before flow cytometry acquisition. Note that, all BRCA1 k.d. cells displayed a higher number of cells with a mean percentage of DNA content above G2 (%>G2).

In what concerns the treatment with doxorubicin (500nM, 4h) we could detect clearly a G2 arrest 24h after the exposure both in SCRAMB and BRCA1 k.d. cells. Despite this fact, BRCA1 k.d. cells displayed a significantly higher percentage of cells with higher DNA contents compared to SCRAMB (approximately 25% compared to 10%) 48h after the treatment (Fig. 23).

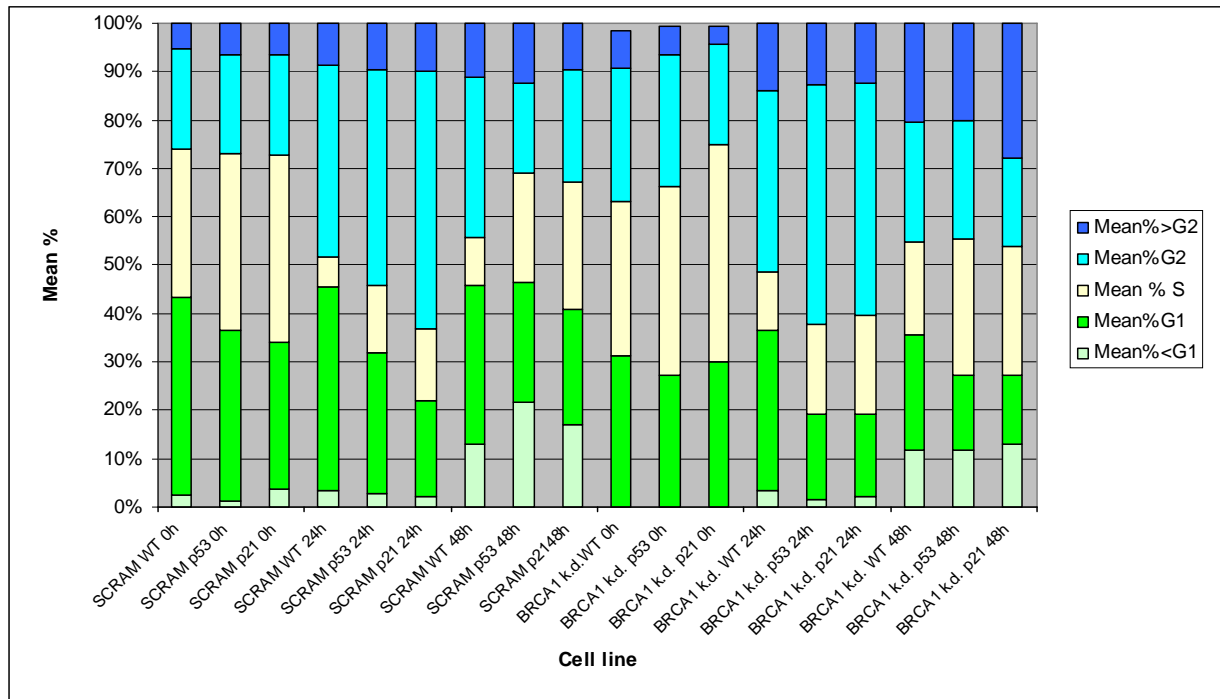


**Figure 23:** Flow cytometry analysis of cell cycle distribution in cells treated with doxorubicin. HCT116 WT, p53 K.O. and p21 K.O. cell lines with BRCA1 k.d. were designated (BRCA1 k.d. WT, BRCA1 k.d. p53 and BRCA1 k.d. p21 respectively). HCT116 WT, p53 K.O. and p21 K.O. cell lines without BRCA1 k.d. were designated (SCRAMB WT, SCRAMB p53 and SCRAMB p21 respectively). Cells growing exponentially were treated with doxorubicin (500nM, 4h) and fixed with ethanol 70% after 1h, 24h and 48h. Note that, BRCA1 k.d. cells displayed a higher number of cells with a mean percentage of DNA content above G2 (%>G2) compared to SCRAMB cells 48h after treatment with doxorubicin.

Regarding irinotecan exposure (3600nM, 12h) we could not distinguish such a considerable difference between SCRAMB and BRCA1 k.d. cells in respect to higher DNA contents 48 hours after the treatment (10% compared to 12% respectively). Furthermore, the G2 arrest we detected in this case started immediately after the treatment (Fig. 24).

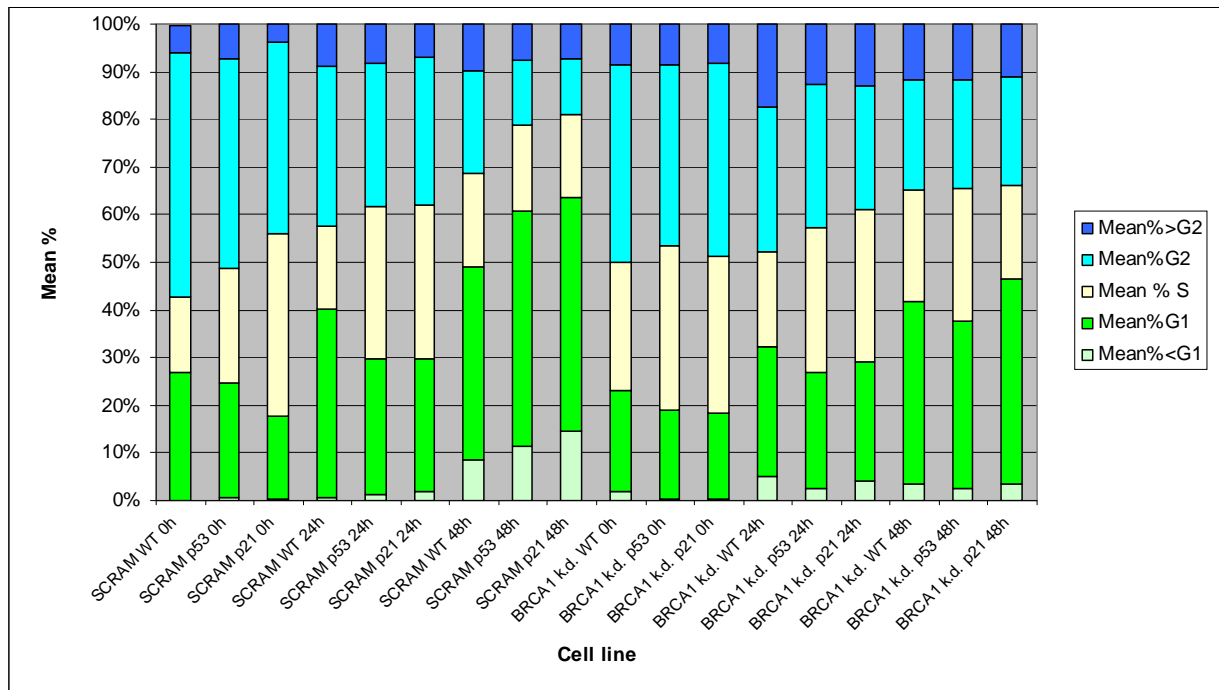
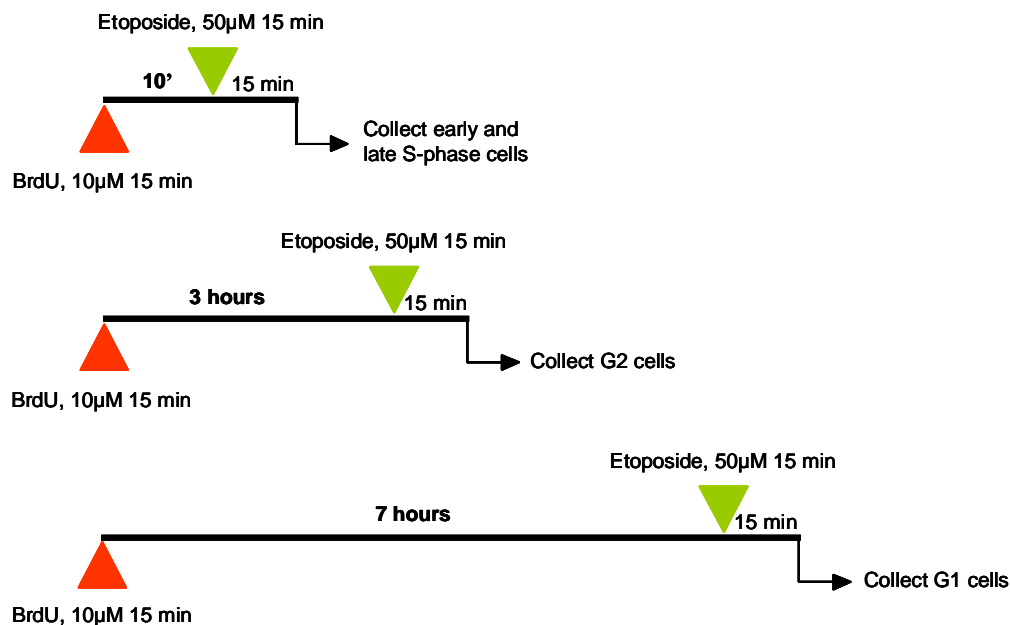


Figure 24: FACS analysis of time course cell cycle distribution in cells treated with irinotecan. HCT116 WT, p53 K.O. and p21 K.O cell lines with BRCA1 k.d. were designated (BRCA1 k.d. WT, BRCA1 k.d. p53 and BRCA1 k.d. p21 respectively). HCT116 WT, p53 K.O. and p21 K.O cell lines without BRCA1 k.d. were designated (SCRAMB WT, SCRAMB p53 and SCRAMB p21 respectively). Cells growing exponentially were treated with irinotecan (360nM, 12h) and fixed with ethanol 70% after 1h, 24h and 48h. Note that, BRCA1 k.d. and SCRAMB cells displayed a similar number of cells with a mean percentage of DNA content above G2 ( $\%>G2$ ) 48h after treatment with irinotecan.

**vi) The amount of H2A.X lesions is independent of the cell cycle phase at which cells were exposed to Etoposide:**

Whenever a cell is exposed to drugs that may harm their genome integrity (genotoxic drugs) and introduce DNA lesions, one of four fates can occur; the cell can repair the lesions, enter the apoptotic program, trigger premature senescence or, finally, become a transformed cell which may lead to tumorigenesis. Surely, it is interesting to understand what in fact happens to cancer cells when patients are treated with topoisomerase II poisons and, whether there is any specific cell cycle phase at which cancer cells are more susceptible to these drugs given that the levels of TOP2 vary along the cell cycle. These levels begin to increase in S phase, and are higher in late S phase than in early S phase; from late S phase to G2 there is also an increase in the levels of TOP2. Our main goal was to evaluate the extension of the DNA lesions (DSBs) induced by TOP2 poisons (etoposide) at different cell cycle phases. To do so, we have measured the total H2AX foci area in cells exposed to etoposide at different cell cycle phases. We have applied a drug exposure scheme based on results obtained from the

cell line characterization. The basis of our approach relied on the replication patterns of cells in S phase and not as could be expected on cell synchronization methods since this last choice usually makes use of pharmacological agents that result in adverse cellular perturbation. For this reason we have used an alternative approach based on the diagram of labelled mitosis (confer cell line characterization results page 14). This is best shown in the schematic depicted bellow (Fig. 25):



**Figure 25:** Use of BrdU-based tag to identify cells that have been damaged at a specific cell cycle phase. To tag cells in early and late S phases, cells were exposed to a BrdU pulse (10µM 15 min) and shortly after (10 min) to etoposide (50µM 15 min). In this way, cells would be exposed to etoposide at early and late S phases and we may analyse them directly by their replication patterns. To tag cells in G2, cells were exposed to a BrdU pulse and subsequently to etoposide (50µM 15 min) after a 3h chase. The 3h chase was chosen because after 3h, cells that were BrdU-pulsed while in late S phase are in G2 upon exposure to etoposide. Thus, using this chase time, the late S pattern can be used as a marker (“tag”) for targeting G2 stage (i.e. cells targeted by etoposide while in G2). To tag cells in G1 we have chosen a 7h pulse chase between the BrdU pulse and the etoposide exposure because after 7h cells that were BrdU-pulsed while in late S are in G1 upon exposure to etoposide. Similarly, we used the late S pattern as a marker for “tagging” G1 stage.

Regarding the whiskers plot, what immediately struck us was how much the H2AX foci area varied within each etoposide exposure stage (Fig. 26). In other words, what we observed was that, within the same cell cycle phase some cells display a large H2AX foci area and others only very small ones; this also holds true to each and all the cell cycle phases analyzed. In the end we could conclude that there was a high dispersion of the H2AX foci area distribution at all cell cycle stages. We have also observed an apparent lack of correlation of between the H2AX foci area and the TOP2 levels although there is more TOP2 in late S phase than in early S-

phase. The control of this experiment was a measure of the H2AX foci area in untreated cells which was similar in both the early and late replication patterns. This allowed us to consider a single control to all the addressed cell cycle phases; the H2AX foci area in the control is thus, considered to be arbitrary level.

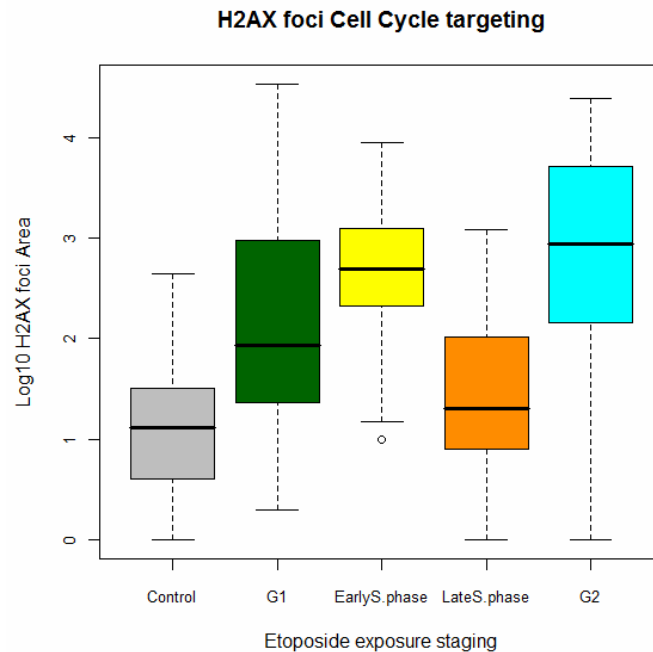


**Figure 26:** Cell cycle targeting of H2AX foci after etoposide exposure. Cells were exposed to etoposide (50 $\mu$ M, 15 min) at each cell cycle phase and the levels of H2AX foci were analysed. Cells were imaged by confocal microscopy using identical image capture settings; 25 cells per experimental group were analysed. Note the high dispersion of the H2AX foci area distribution at all cell cycle stages.

Moreover, it is important to notice that we only measured 25 nuclei for each experimental group and therefore, concerning variations between the different groups, these research experiments shall be strengthened in the future by additional measurements.

**vii) Etoposide treatment causes a decrease in histone H3 K9 tri-methylation in addition to an increase in heterochromatin protein 1 $\alpha$ :**

The association of senescence with alterations in the chromatin structure and in the nuclear size (confer introduction page 4) together with the increase in the nuclear size observed after treatment with etoposide prompted us to ask whether this increase in the nuclear size could be caused by an increase in chromatin decondensation. To test this hypothesis we evaluated the expression levels of Histone H3 tri-methyl K9 (H3K9me3) which is currently seen as a marker of silenced chromatin and of heterochromatin protein-1 $\alpha$  (HP-1 $\alpha$ ) [56] which is a major constituent of heterochromatin. In this experiment cells were treated either 15 or 30 min with

etoposide 50  $\mu$ M and then 1, 2 or three days after each treatment total protein extracts were collected to assess HP1 $\alpha$  and H3K9me3 levels. The reason behind the 30 min exposure is simple: with immunofluorescence experiments, we observed that after 30 min exposure, almost all cells display larger nuclei; this allowed us to analyse a nearly pure population of cells with large nuclei (Fig. 27).

With respect to HP1 $\alpha$  we observed an increase two days after treatment with etoposide 50  $\mu$ M, 15 min followed by a decrease in the third day which probably shows that cells have started to recover. After treatment with etoposide 50  $\mu$ M, 30 min we observed an increase in HP1 $\alpha$  both in the second and third day after exposure. To assess whether HP1 $\alpha$  is associated or not to the chromatin, we should do a detergent assay.

H3K9me3, on the other hand seems to be decreased on day 2 and 3 after treatment with both etoposide 50  $\mu$ M, 15 min and 30 min. This fact shows as, undoubtedly, that etoposide treatment leads gradually to chromatin derepression in HCT116 WT cells.

These results are to be further explored and suggest that alterations in chromatin composition may be an early marker of the senescent state commitment. It would be of great interest to see if these expressions patterns are maintained in BRCA1-depleted cells.

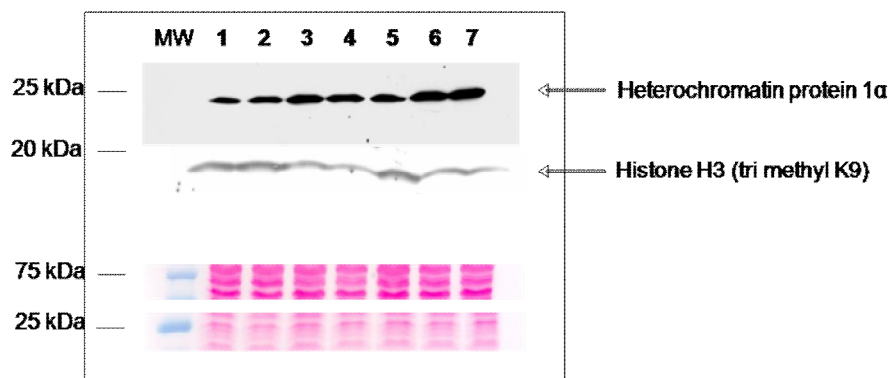


**Figure 27:** Western blot experiment to evaluate the expression levels of HP1 $\alpha$  and H3K9me3 in HCT116 WT control (lane 1); HCT116 WT treated with etoposide 50  $\mu$ M 15 min, 1 day, 2 days and 3 days after exposure (lane 2, lane 3 and lane 4 respectively); HCT116 wt treated with etoposide 50  $\mu$ M 30 min, 1 day, 2 days and 3 days after exposure (lane 5, lane 6 and lane 7 respectively). MW, molecular weight maker. There was concomitantly an increase in HP1 $\alpha$  and a decrease in H3K9me3 after treatment with etoposide.

## V) Conclusion

DNA topoisomerase II is a ubiquitous enzyme, essential for the survival of all eukaryotic organisms. This enzyme plays a critical role in almost every aspect of the DNA metabolism and is also crucially important in the removal of knots and linkages between daughter chromatids



such that entangled chromosomes can be separated at mitosis. Topoisomerase II has, therefore become the main target of several antitumor therapies even though the exact mechanism of cell killing remains elusive. In an effort to provide further insight into Topoisomerase II-mediated DNA damage, we proposed to study the role not only of BRCA1 but also of some chromatin structure regulators in the cellular outcome following exposure to Topoisomerase drugs. We could conclude that BRCA1 plays a role in the senescent outcome after exposure to Topoisomerase-II poisons. It was also observed that BRCA1 depletion led to an increase in the number of cells with high DNA contents (above 4N). The possible connection between increase in ploidy (genomic instability) and senescence is still speculative, but warrants future insight.

In addition, we have addressed if there was any quantitative correlation between H2AX foci area and cell cycle stage exposure to Topoisomerase II poison etoposide. Despite the small size of the samples it was noticeable that the DNA damage foci area had no apparent relation with the cell cycle stage at which cells were exposed to the poison. Nevertheless, we shall continue to extend our measurements in order to confirm this initial result.

Furthermore, we decided to check the heterochromatin status of the cells, especially those that exhibit larger nuclei for they will probably correspond to pre-senescent nuclei [57]. Indeed, it was visible a decrease in the tri-methylated form of histone H3 accompanied by an increase in the amount of HP1 $\alpha$ . This latter evidence can be justified either by an increase in chromatin condensation or in free HP1 $\alpha$ . In order to establish that etoposide exposure leads to an increase in the chromatin condensation state of cells we need to reject the other possibility in future experiments.

To conclude, there are a few hypotheses we can advance, based on the results obtained through this research. First of all, we can picture a feasible pathway in which exposure to Topoisomerase II poisons causes DNA double-strand breaks that will not be properly repaired due to BRCA1 depletion. This fact increases genomic instability that subsequently leads to an increase in the cellular senescent outcome. Nonetheless, we can go further and boldly suggest a more direct role of BRCA1 in senescence, in which a novel pathway comprising this protein would be the *bona fide* cause of the cellular senescent outcome increase in cells that were depleted of BRCA1. If we take into account the HP1 $\alpha$  and H3K9me3 results and the fact that BRCA1 interacts with several proteins involved in chromatin modifications, we can also hypothesize that BRCA1 depletion may cause a defect in heterochromatin maintenance which will, in turn, favour the senescent outcome. In any case, it would be scientifically relevant to test this latter hypothesis in further studies.

## X. References:

- [1] Wang, J. C.; 1996; *DNA topoisomerases*; Annu. Rev. Biochem.; 65, 635-692.
- [2] Froelich-Ammon, S.J., Osheroff, N., 1995, *Topoisomerase Poisons: Harnessing the Dark Side of Enzyme Mechanism*, J. Cell. Biol., 270:37, 21429-21432
- [3] Wang, J.C.; 2002, *Cellular roles of DNA topoisomerases: a molecular perspective*, Mol. Cell. Biol., 3, 430-440
- [4] Classen, S. *et al.*, 2003, *Structure of the topoisomerase II ATPase region and its mechanism of inhibition by the chemotherapeutic agent ICRF-187*, PNAS, 100:19, 10629-10634
- [5] Champoux, J.J., 2001, *DNA Topoisomerases: Structure, Function and Mechanism*, Annu. Rev. Biochem., 70, 369-413
- [6] McClendon, K.A. *et al.*, 2005, *Human Topoisomerase II $\alpha$  Rapidly Relaxes Positively Supercoiled DNA*, J. Biol. Chem., 280:57, 39337-39345
- [7] Meyer K.N. *et al.*, 1997, *Cell Cycle-coupled Relcoation of Types I and II Topoisomerases and Modulation of Catalytic Enzyme Activities*, J. Cell. Biol., 136:4, 775-788
- [8] Burden, A. and Osheroff, N., 1998, *Mechanism of action of eukaryotic topoisomerase II and drugs targeted to the enzyme*, Biochimica et Biophysica Acta 1400, 139-154
- [9] Kellner, U. *et al.*, 2002, *Culprit and victim – DNA topoisomerase II*, Lancet Oncol, 3, 235-243
- [10] Agostinho M. *et al.*, 2004, *Human Topoisomerase II $\alpha$ : Targeting to Subchromosomal Sites of Activity during Interphase and Mitosis*, Mol. Biol. Cell., 15, 2388-2400
- [11] Larsen, K.A. *et al.*, 2003, *From DNA damage to G<sub>2</sub> arrest: the many roles of topoisomerase II*, Prog. in Cell Cycle Res., 5, 295-300
- [12] Watt, P. M., Hickson, D. I., 1994, *Structure and function of type II DNA topoisomerases*, Biochem. J., 303, 681-695
- [13] Germe, T., Hyrien, O., 2005, *Topoisomerase II–DNA complexes trapped by ICRF-193 perturb chromatin structure*, EMBO reports, 6:8, 729-735
- [14] Ting, N.S.Y., Lee, WH., 2004, *The DNA double-strand break response pathway: becoming more BRCAish than ever*, DNA Repair, 3, 935-944
- [15] Jackson, S.P., 2002, *Sensing and repairing DNA double-strand breaks*, Carcinogenesis, 23:5, 687-696
- [16] Zhou, B-B. S., Elledge, S.J., 2000, *The DNA damage response: putting checkpoints in perspective*, Nature, 408, 433-439
- [17] O'Driscoll, M., Jeggo, P.A., 2006, *The role of double-strand break repair-insights from human genetics*, Nat. Rev. Gen., 7, 45-54

- [18] Petrini, J.H.J. and Stracker, T.H., 2003, *The cellular response to DNA-double strand breaks: defining the sensors and mediators*, Trends Cel. Biol., 13:9, 458-462
- [19] Bakkenist, C.J. and Kastan, M.B., 2003, *DNA damage activates ATM through intermolecular autophosphorylation and dimer dissociation*, Nature, 421, 499–506
- [20] Liu, J-S., *et al.*, 2006, *DNA Damage-Induced RPA Focalization is Independent of  $\gamma$ -H2AX and RPA Hyper-Phosphorylation*, JCB, 99, 1452-1462
- [21] Fernandez-Capetillo, O., *et al.*, 2004, *H2AX: the histone guardian of the genome*, DNA Repair, 3, 959-967
- [22] Lavin, M.F., 2008, *Ataxia-telangiectasia: from a rare disorder to a paradigm for cell signalling and cancer*, Nat. Rev. Mol. Cell Biol., 9, 759-768
- [23] Thompson, L.H. and Limoli, C.L., *Origin, Recognition, Signaling and Repair of DNA Double-Strand Breaks in Mammalian Cells* In: Caldecott, K.M, *Eukaryotic DNA Damage Surveillance and Repair*, Caldecott, K. W., 2004, cap. 6, p. 107-146
- [24] Zhou, B-B. S., Bartek, J., 2004, *Targetting the checkpoint kinases: chemosensitization versus chemoprotection*, Nat. Rev. Can., 4, 216-225
- [25] Foray, N. *et al.*, 2003, *A subset of ATM- and ATR-dependent phosphorylation events requires the BRCA1 protein*, EMBO J., 22:11, 2860-2871
- [26] Cohn, M.A., D'Andrea, A.D., 2008, *Chromatin Recruitment of DNA Repair Proteins: Lessons from the Fanconi Anemia and Double-Strand Break Repair Pathways*, Mol. Cell, 32, 306-312
- [27] Helleday T. *et al.*, 2008, *DNA repair pathways as targets for cancer therapy*, Nat. Rev. Cancer, 8, 193-204
- [28] Pardo, B. *et al.*, 2009, *DNA double-strand break repair: how to fix a broken relationship*, Cell. Mol. Life Sci., 1-18
- [29] Shrivastav, M. *et al.*, 2008, *Regulation of DNA double-strand break repair pathway choice*, Cell Res., 18, 134-147
- [30] Khanna K.K., Jackson, S.P., 2001, *DNA double-strand breaks: signaling, repairing and the cancer connection*, Nat. Gen., 27, 247-254
- [31] Zhang, J., Powell, S.N., 2005, *The role of the BRCA1 tumor suppressor in DNA double-strand break repair*, Mol. Cancer Res., 3:10, 531-539
- [32] Deng, CX., Wang, RH., 2003, *Roles of BRCA1 in DNA damage repair: a link between development and cancer*, Hum. Mol. Gen., 12:1, R113-R123

- [33] Ishida, R., *et al.*, 1994, *Inhibition of DNA topoisomerase II by ICRF-193 induces polyploidization by uncoupling chromosome dynamics from other cell cycle event*, *J. Cell Biol.*, 126, 1341–1351
- [34] Kastan, M.B. and Barket, J., 2004, *Cell-cycle checkpoints and cancer*, *Nature*, 432, 316–323
- [35] Jackson, S.P. *et al.*, 2003, *A DNA damage checkpoint response in telomere-initiated senescence*, *Nature*, 426, 194–198
- [36] Cao, L. and Finkel, T., 2006, *Cancer gets the Chk'ered flag*, *Nat. Med.*, 12, 1354–1356
- [37] Funayama, R. and Ishikawa, F., 2007, *Cellular senescence and chromatin structure*, *Chromosoma*, 116, 431–440
- [38] Narita, M. *et al.*, 2003, *Rb-mediated heterochromatin formation and silencing of E2F target genes during cellular senescence*, *Cell*, 113:6, 703–716
- [39] Oberdoerffer, P. and Sinclair, D.A., 2007, *The role of nuclear architecture in genomic instability and ageing*, *Nat. Rev. Mol. Cell Biol.*, 8, 692–702
- [40] Ogryzko, V. V., *et al.*, 1996, *Human fibroblast commitment to a senescence-like state in response to histone deacetylase inhibitors is cell cycle dependent*, *Mol. Cell Biol.*, 16, 5210–5218
- [41] Qinong, Y *et al.*, 2001, *BRCA1-induced large-scale chromatin unfolding and allele-specific effects of cancer-predisposing mutations*, *JCB*, 155:6, 911–921
- [42] Lou, Z. *et al.*, 2005, *BRCA1 participates in DNA decatenation*, *Nat. Struct. Mol. Biol.*, 12:7, 589–593
- [43] Campisi, J., 2001, *Cellular senescence as a tumor-suppressor mechanism*, *Trends Cell Biol.*, 11:11, S27–S31
- [44] Beauséjour, C.M. *et al.*, 2003, *Reversal of human cellular senescence: roles of the p53 and p16 pathways*, *EMBO J.*, 22, 4212–4222
- [45] , J. and d'Adda di Fagagna, F., 2007, *Cellular senescence: when bad things happen to good cells*, *Nat. Rev. Mol. Cell Biol.*, 8, 729–740
- [46] Moffat, J. *et al.*, 2006, *A Lentiviral RNAi Library for Human and Mouse Genes Applied to an Arrayed Viral High-Content Screen*, *Cell*, 124, 1283–1298
- [47] Baserga, R., *Cell growth and division, a practical approach*, In: Rickwood, D. and Hames B.D., *The practical approach series*, Rickwood, D. and Hames B.D., cap. 1, p. 1–15, IRL Press
- [48] Mitchison, J.M., *The biology of the cell cycle*, In: Mitchison, J.M., *European molecular biology laboratory hiedelberg*, 1971, cap. 2, p. 25–58, Cambridge University Press

- [49] Ferreira, J. *et al.*, 1997, *Spatial Organization of Large-Scale Chromatin Domains in the Nucleus: A Magnified View of Single Chromosome Territories*, 139:7, 1597-1610
- [50] Mather, J.P., Roberts, P.E., 1998, *Introduction to Cell and Tissue Culture: Theory and Technique*, Plenum Press
- [51] Plumb, J.A., *Cell Sensitivity Assays: The MTT Assay*, In: Langdon, S.P., *Cancer cell culture methods and protocols*, 2004, cap 14, p. 165-171, Humana Press
- [52] Plumb, J.A., *Cell Sensitivity Assays: Clonogenic Assay*, In: Langdon, S.P., *Cancer cell culture methods and protocols*, 2004, cap 13, p. 159-165, Humana Press
- [53] Clarke, D.J. *et al.*, 1993, *Topoisomerase II inhibition prevents anaphase chromatid segregation in mammalian cells independently of the generation of DNA strand breaks*, J. Cell Sci., 105, 563–569
- [54] Chen, M. and Beck, W.T., 1995, *Differences in inhibition of chromosome separation and G2 arrest by DNA topoisomerase II inhibitors merbarone and VM-26*, *Cancer Res.*, 55, 1509–1516
- [55] Cortés, F. and Pastor, N., 2003, *Induction of endoreduplication by topoisomerase II catalytic inhibitors*, *Mutagenesis*, 18:2, 105-112
- [56] Eskeland, R. *et al.*, 2007, *HP1 Binding to Chromatin Methylated at H3K9 Is Enhanced by Auxiliary Factors*, *Mol. Cell. Biol.*, 27:2, 453-465
- [57] Mocali, A. *et al.*, 2005, *The Comet Assay Approach to Senescent Human Diploid Fibroblasts Identifies Different Phenotypes and Clarifies Relationships Among Nuclear Size, DNA Content, and DNA Damage*, *J. of Geront.*, 60A:6, 695-701
- [58] Montecucco, A., Biamonti, G., 2007, *Cellular response to Etoposide treatment*, *Cancer Letters*, 252, 9-18
- [59] Lobrich, M., Jeggo, P.A., 2007, *The impact of a negligent G2/M checkpoint on genomic instability and cancer induction*, *Nat. Rev. Can.*, 7, 861-869
- [60] Deng, Y. *et al.*, 2008, *Telomere dysfunction and tumour suppression: the senescence connection*, *Nat. Rev. Can.*, 8, 450-458

## XI. Annex

**Figure 1:**

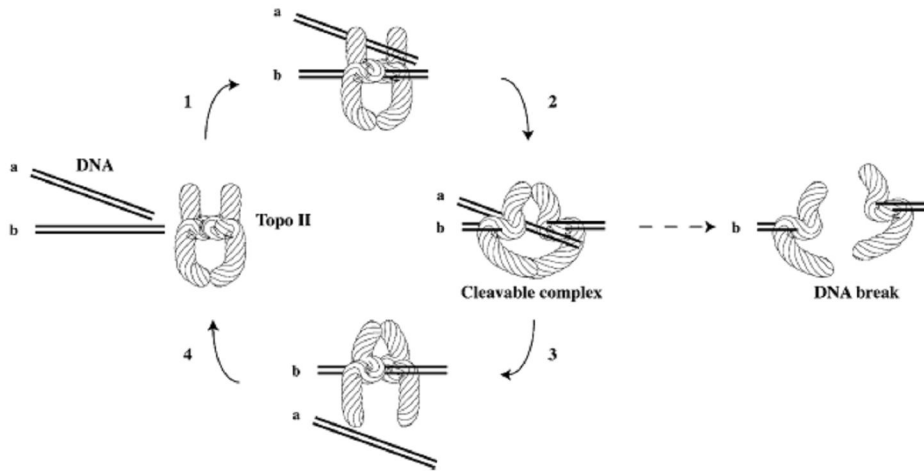


Figure 1: Catalytic mechanism of type II DNA topoisomerases [58].

**Figure 2:**

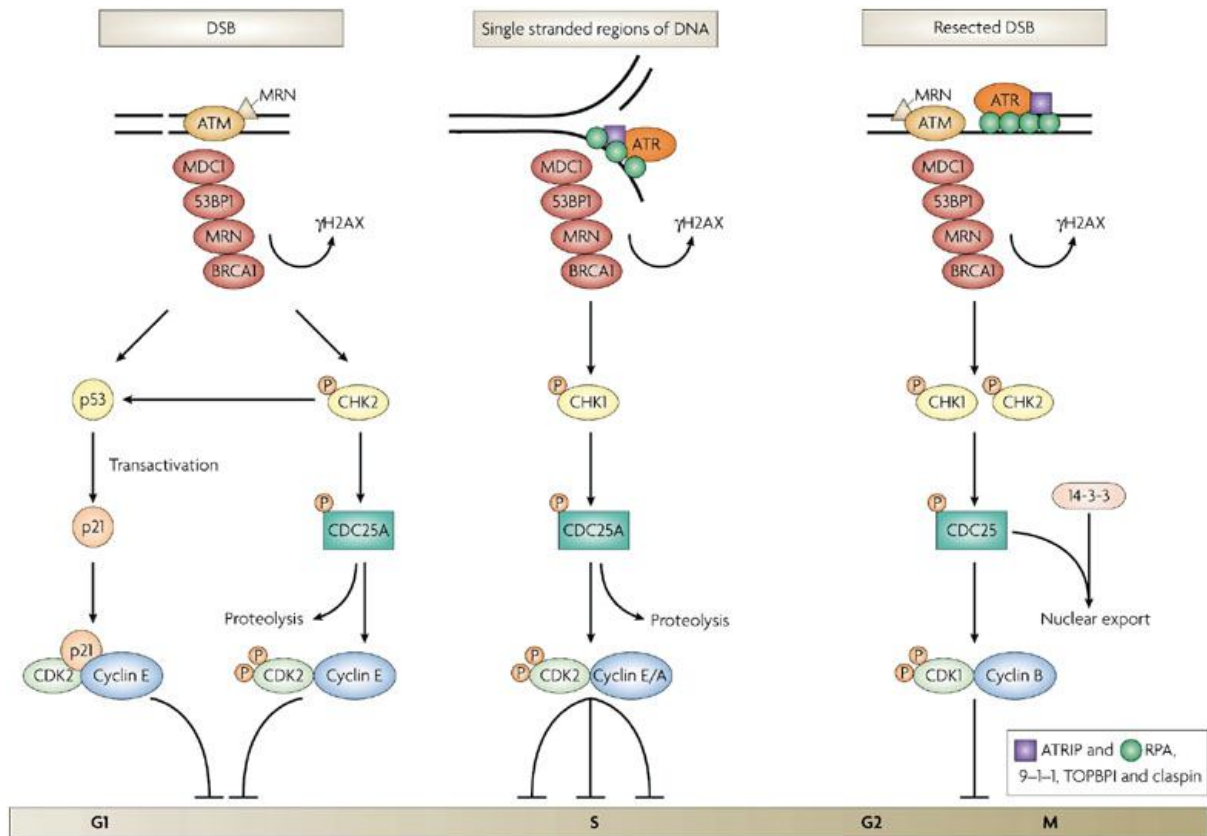
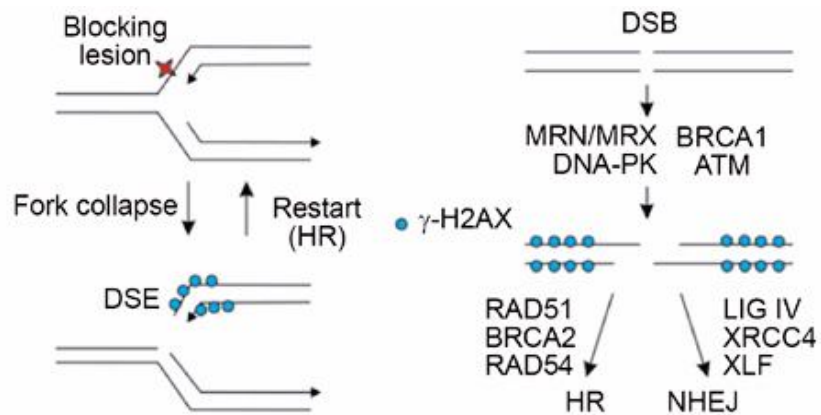


Figure 2: Schematic illustration of the DNA damage response [59]. Either ATM or ATR can activate signal transduction pathways, which respond to DSBs or to single-stranded regions respectively. The signalling pathways involve mediator proteins that amplify the signal (MDC1, 53BP1, MRN, BRCA1), transducer kinases (CHK1 and CHK2) and effector proteins. There is considerable overlap between ATM and ATR phosphorylation substrates. Two G1/S checkpoints are dependent on ATM signalling.

**Figure 3:**



**Figure 3:** DNA DSBs repair pathways [29]. Replication forks can stall and may collapse when they encounter a blocking lesion. This will induced H2AX phosphorylation in the site of damage. Fork restart usually involves HR proteins. Frank double strand breaks (two broken ends) may be repaired either by NHEJ or by HR.

**Figure 4:**

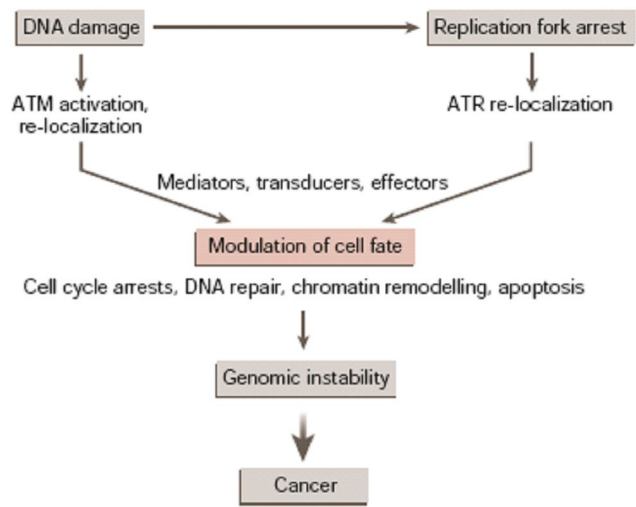


**Figure 4:** General scheme of DNA damage or replication fork arrest responses: the impact on cell fate, cancer development and genomic instability [34].

**Figure 5:**

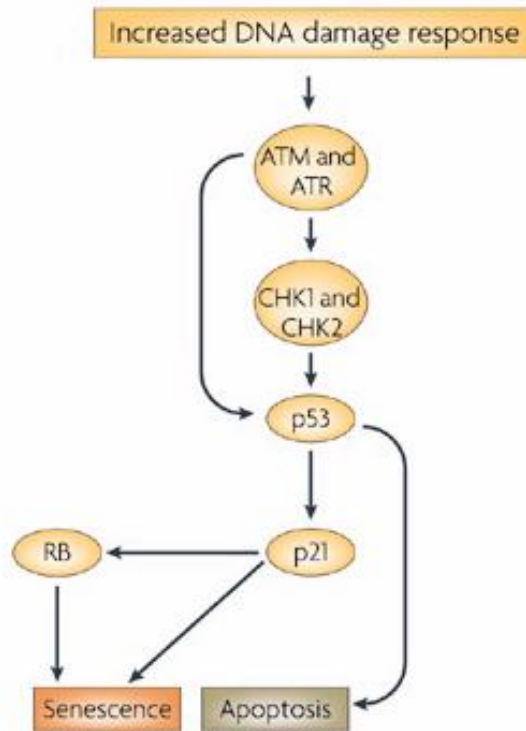
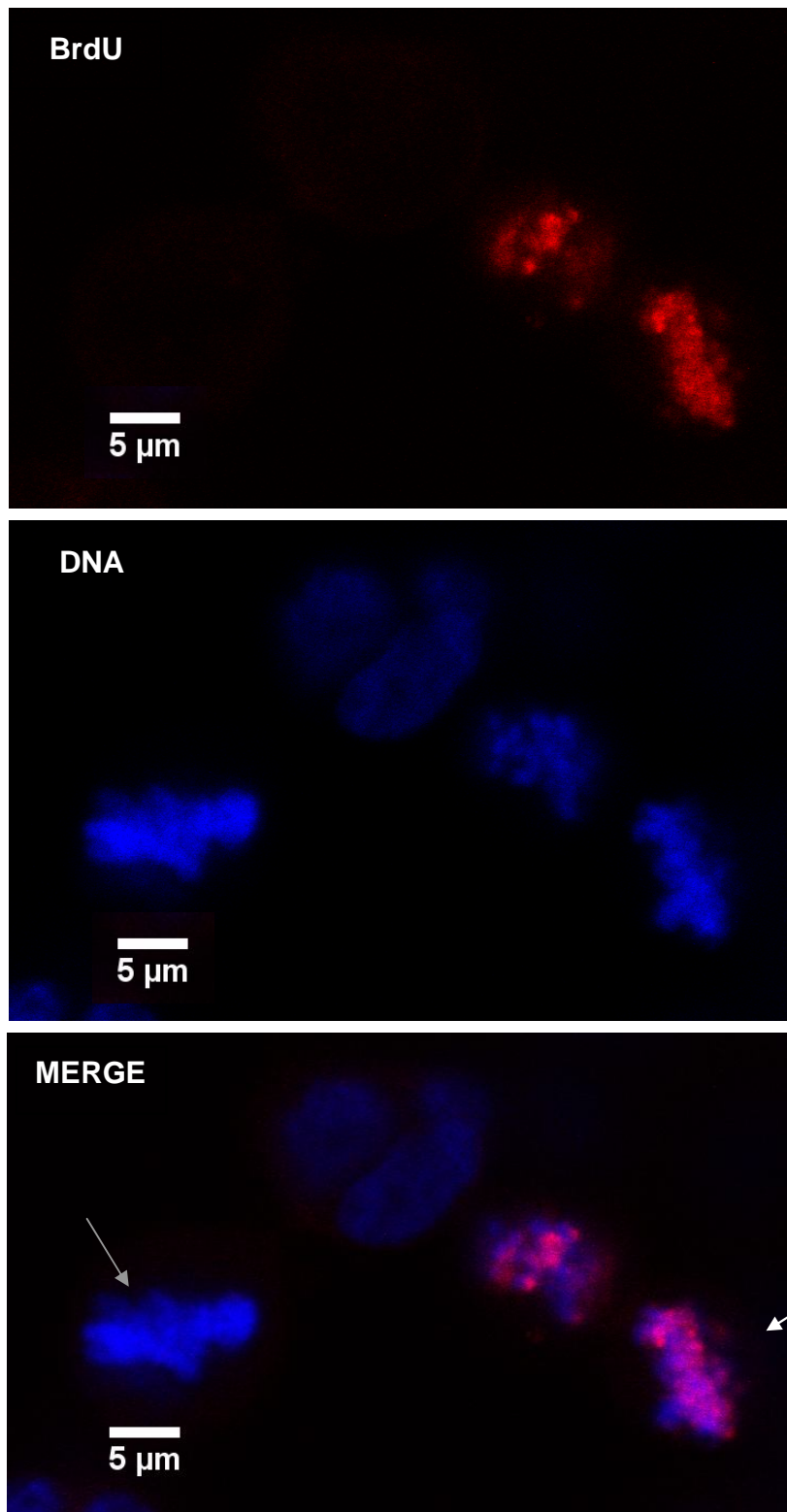


Figure 5: P53-dependent senescence, *adapted from* [60]. An increased DNA damage response results in p53 phosphorylation which transcriptionally upregulates genes that mediate either apoptosis or cellular senescence to inhibit tumorigenesis.



**Figure 9:**



**Figure 9:** BrdU labelled mitosis. Cells were stained for BrdU and DNA was stained with DAPI (*bar*, 5µm). Note that BrdU and DAPI colocalize at the metaphasic plate (white arrow). DAPI staining of a metaphasic plate that does not stain for BrdU (grey arrow).

**Diagram 1:**

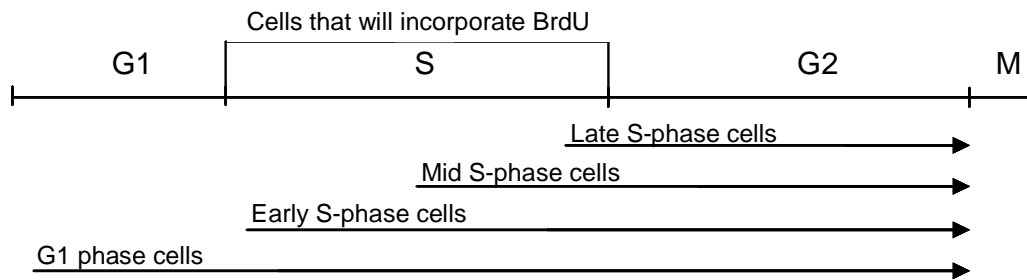


**Diagram 1:** Schematic of the labelled mitosis method. Cells that were in late S phase when BrdU-pulsed will be the first mitotic BrdU positive (+) cells. Similarly, cells that were in G1 phase when BrdU-pulsed will be the last mitotic BrdU positive (+) cells of the first cell cycle. A second cell cycle will initiate when the original late S phase cells pass through G2 and enter mitosis for the second time.

**Figure 15:**

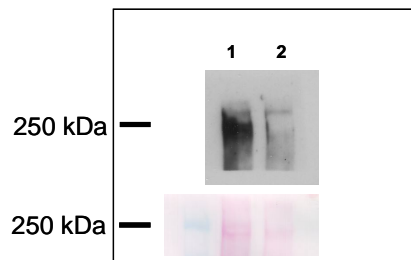
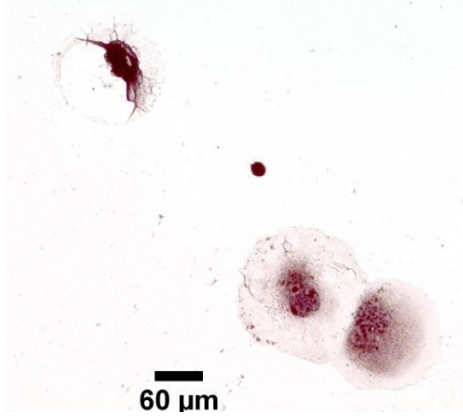


**Figure 15:** Western blotting experiment to evaluate the level of BRCA1 depletion. HCT116 WT SCRAMB, lane 1 and HCT116 WT BRCA1 k.d., lane 2.

**Figura 16:**

**A)**



**B)**

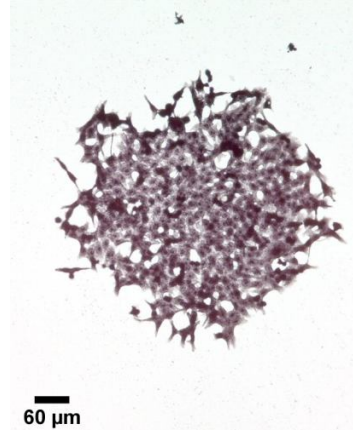


Figure 16: Haematoxylin staining of HCT116 WT BRCA1 k.d. cells. *A*, HCT116 WT BRCA1 k.d. cells treated with doxorubicin (500nM, 4h). Note the size of the senescent cell (black arrow). *Bar*, 60  $\mu$ m. *B*, HCT116 WT BRCA1 k.d. cells (control, no treatment). Note a large colony of regular cells. *Bar*, 60  $\mu$ m

**Figura 19:**

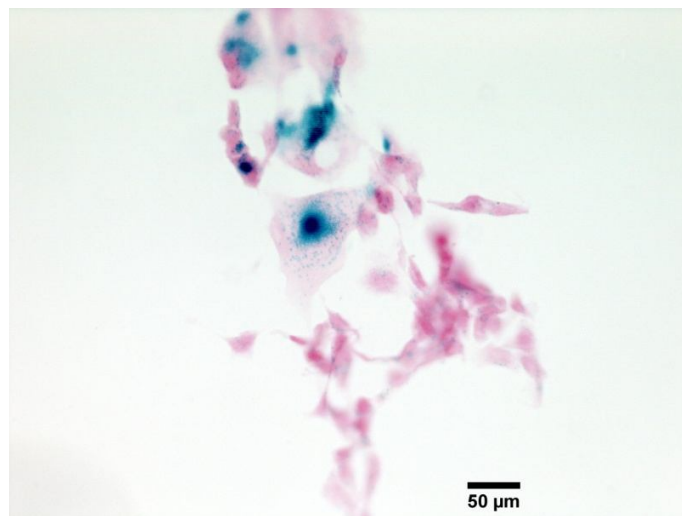


Figure 19: Senescence-associated  $\beta$ -galactosidase staining of HCT116 WT BRCA1 k.d. cells treated with doxorubicin (500nM, 4h). *Bar*, 50  $\mu$ m.